STRUCTURAL STUDIES OF IRON–SULFUR PROTEINS

JOHN C. M. TSIBRIS AND ROBERT W. WOODY*

Department of Chemistry and Chemical Engineering, University of Illinois, Urbana, Illinois, 61801 (U.S.A.)

CONTENTS

A. Introduction
   (i) Scope
   (ii) Classification of iron–sulfur proteins
B. 1–Fe Proteins
   (i) Chemistry
   (ii) Optical spectroscopy
   (iii) EPR
   (iv) X-ray diffraction
   (v) Discussion
C. 2Fe–2S* proteins
   (i) Chemistry
   (ii) Optical spectroscopy
   (iii) EPR, ENDOR and magnetic susceptibility
   (iv) Mössbauer spectroscopy
   (v) NMR
   (vi) Discussion
D. 4Fe–4S* proteins
   (i) Chemistry
   (ii) Optical spectroscopy
   (iii) EPR and magnetic susceptibility
   (iv) Mössbauer spectroscopy
   (v) X-ray diffraction
   (vi) Discussion
E. nFe–nS* proteins
   (i) Chemistry
   (ii) Optical spectroscopy
   (iii) EPR and magnetic susceptibility

* Present address: Chemistry Department, Arizona State University, Tempe, Ariz. 85281, U.S.A.

A. INTRODUCTION

(*i*) *Scope*

Iron–sulfur proteins contain at least one iron atom coordinated by one or more sulfur ligands. These proteins participate in many biologically important reactions and present intriguing structural problems. Most of these proteins have been referred to previously as "non-heme iron" proteins. This nomenclature largely reflected the biochemists' long preoccupation with iron–porphyrin proteins. We prefer the more descriptive term "iron–sulfur" proteins.

Iron–sulfur proteins have been recognized as a distinct class only in the last decade, although some members of this group, especially the iron–sulfur flavoproteins, were discovered and extensively studied much earlier. Iron–sulfur proteins participate, for example, in photosynthesis (ferredoxins), nitrogen fixation (nitrogenases), hydroxylation of steroids and other terpenes (adrenodoxin and putidaredoxin) and electron transport (iron–sulfur flavoproteins). A few members of this class (most rubredoxins and high-potential iron proteins (HiPIP)) have not yet been associated with specific biological functions.

Because of their involvement in so many fundamental biological processes,

CD	= circular dichroism	HiPIP	= high-potential iron proteins
DPNH	= diphosphopyridine nucleotide (reduced)	NMR	= nuclear magnetic resonance
		ORD	= optical rotatory dispersion
ENDOR	= electron nuclear double resonance	S*	= acid-labile sulfur
EPR	= electron paramagnetic resonance	TCA	= trichloroacetic acid
FAD	= flavin adenine dinucleotide (oxidized)	TPNH	= triphosphopyridine nucleotide (reduced)
FADH$_2$	= flavin adenine dinucleotide (reduced)		

iron–sulfur proteins are obviously of interest to biochemists. They have also attracted the attention of many inorganic and physical chemists and physicists because of their novel structural and spectroscopic properties and the opportunity they provide for application of a wide range of powerful physical techniques to a biologically significant problem.

The purpose of this review is to acquaint coordination chemists with the structural problems posed by iron–sulfur proteins and the progress which has been made toward their solution. We have emphasized those studies which relate directly to the elucidation of the structure and bonding of the iron–sulfur center in these systems. Several recent reviews[29,72,85] of this area should be referred to for more details on the biochemical aspects of iron–sulfur proteins.

It is now clear that there are various types of iron–sulfur proteins. In general iron-containing proteins can be placed in three broad categories:

(I)—Proteins in which the iron is bound (covalently or non-covalently) to the proteins as an iron–porphyrin complex (heme proteins). This includes such familiar proteins as hemoglobin and the cytochromes. There is a growing body of evidence that at least two types of heme proteins contain iron–sulfur bonds, i.e., a sulfur-containing amino acid side-chain acts as an additional ligand for the iron, occupying one of the two coordination sites not taken up by the porphyrin. In cytochrome c, the work of Harbury and his co-workers[56,57] has pointed to the thioether sulfur of methionine as one of the extra ligands of iron. This is consistent with, but not yet proven by, X-ray diffraction studies[42] of cytochrome C. The work of Yu and Gunsalus[155] indicates that the thiol group of cysteine is an iron ligand in cytochrome P-450. Bayer et al.[9] have shown that thiol complexes of hemoglobin have EPR signals resembling those of P-450. Although these systems belong to the iron–sulfur protein class by our definition of the term, we do not consider them here because the presence of the porphyrin confers upon them properties quite different from those of the remaining iron–sulfur proteins.

(II)—Proteins in which the iron is bonded to one or more sulfur ligands, and in which a porphyrin ligand is absent. This class includes the rubredoxins, ferredoxins, iron–sulfur flavoproteins, etc., with which this review is concerned. Within this class, a number of distinct types are recognizable, as will be discussed below.

(III)—Proteins in which the iron is bonded to oxygen and/or nitrogen ligands and which lack porphyrin ligands. Many proteins in this group (transferrin, ferritin) appear to function as storage or transport proteins[47,87]. Some which we tentatively include in this class may in fact turn out to have iron–sulfur bonds and therefore properly belong to class II, e.g., the dioxygenases[60]. Dioxygenases activate molecular oxygen and catalyze its incorporation in many types of molecules. Since there is no definite evidence that iron–sulfur bonds occur in these systems, and their spectroscopic properties are quite different from typical iron–sulfur proteins, we will not consider them in this review.

(ii) Classification of iron–sulfur proteins

The members of class II can be further subdivided according to the number of irons per protein molecule and the presence of other prosthetic groups. Except for the members of the first subdivision, all of these proteins contain "acid-labile" or "inorganic" sulfide, which we will denote by S*, in an amount equivalent to their iron content.

(*a*) 1-Fe proteins, *e.g.*, rubredoxins.

(*b*) 2Fe–2S* proteins, *e.g.*, green plant ferredoxins, adrenodoxin, putidare-doxin.

(*c*) 4Fe–4S* proteins, *e.g.*, HiPIP.

(*d*) *n*Fe–*n*S* proteins (reported values of *n* range from 6–8), *e.g.*, bacterial ferredoxins.

(*e*) Iron–sulfur flavoproteins, *e.g.*, xanthine oxidase, aldehyde oxidase, succinic dehydrogenase, *etc.* Proteins containing $(Fe-S^*)_n$ in addition to flavin and, in some cases, molybdenum.

(*f*) Nitrogenases: there appear to be two Fe–S*-containing components involved in N_2 fixation, one of which also contains molybdenum.

In the following sections, we will consider each of these types of iron–sulfur proteins.

B. 1-Fe PROTEINS (RUBREDOXINS)

(i) Chemistry

Rubredoxins are found in numerous anaerobic[81,104] and aerobic bacteria[117]. They have a reddish color, hence their name, and contain one atom of iron per molecule of protein but no acid-labile sulfur. They have a molecular weight of *ca.* 6,000, except for the rubredoxin from *Pseudomonas oleovorans* which has one iron atom per *ca.* 12,800 mol. weight[32].

The amino acid sequences of two rubredoxins have been determined[3–5]. The four cysteines are found in pairs, separated by two amino acids in each case.

In biological reactions rubredoxins can substitute for ferredoxins from various sources but they are not known (except[117] for rubredoxin from *Ps. oleovorans*) to catalyze a reaction of their own. They are auto-oxidizable in air and can be reduced by dithionite or by TPNH or DPNH in the presence or absence of ferredoxin reductases. Rubredoxin from *Clostridium pasteurianum* undergoes[81] a reversible one-electron oxidation and reduction with a redox potential of about −57 mV.

Lovenberg and Williams[81] removed the iron from rubredoxin by precipitation of the protein with trichloroacetic acid. The resulting aporubredoxin shows

no absorption in the visible. By treating aporubredoxin with an excess of a sulf-hydryl reagent, (2-mercaptoethanol or dithiothreitol) and Fe^{3+} or Fe^{2+}, a fully reconstituted rubredoxin can be obtained with properties identical to those of the native protein. Addition of mercurials to rubredoxin[2,81] leads also to a loss of the visible spectrum and four cysteine residues can be titrated. The rate of this slow reaction increases with decreasing size of mercurial, i.e., mercuric acetate is much faster than sodium mersalyl[81]. The loss in absorbancy (e.g., at 490 nm) occurs at the same rate as the reaction of mercurial with the four SH groups, suggesting that all four SH groups are involved as metal–protein ligands. In aporubredoxin less than four cysteines are titratable, probably because of partial oxidation of SH groups during the preparation of the apoprotein. Most probably this partial oxida-tion of SH groups is the reason a sulfhydryl reagent is required for the reconstitu-tion of the aporubredoxin with Fe^{3+}.

Attempts to alkylate rubredoxin[2] with iodoacetic acid in the presence of 5M guanidinium hydrochloride were unsuccessful. It seems therefore that the iron in the molecule protects the sulfhydryl groups from alkylation. However, four moles of iodoacetamide react per mole of aporubredoxin when incubated in the presence of 8M urea and 0.5M 2-mercaptoethanol[81], illustrating that the SH groups are available for reaction only after removal of the iron. In the presence of 2-mercapto-ethanol an exchange between exogenous iron and iron of rubredoxin occurs[81] having a sharp pH optimum, around pH 7.

Bachmayer et al.[5] have investigated the possibility that amino acids other than cysteine act as iron ligands in rubredoxin. The amino acid sequences of apo-rubredoxin from several bacteria are now known[149]. This facilitates the use of chemical reagents specific for certain amino acids to study the binding of their functional groups. Bachmayer et al. were able to eliminate the α-amino and the thioether group of the N-terminal methionine and the two lysines as potential iron ligands. They also found that modification of tyrosine and tryptophan resi-dues in aporubredoxin abolishes its capacity to recombine with iron, and suggested that one tyrosine and one tryptophan serve as ligands, in addition to the four cysteines. Chemical modification procedures of this type are useful for establishing the non-involvement of certain groups, but cannot distinguish between the possi-bility that altering a particular residue may destroy recombination capacity by (a) blocking a ligand or (b) preventing proper refolding of the protein chain through some other mechanism.

(ii) Optical spectroscopy

The absorption spectra of rubredoxins from various species are very simi-lar[1,80,104,117]. The oxidized state gives prominent maxima at 490, 380 and 280 nm, and more or less distinct shoulders at about 560 and 350 nm. Upon chemical or enzymatic reduction, the absorption spectrum is strikingly altered. The reduced

protein shows no visible absorption bands, but has maxima at 330, 310 and 275 nm, as well as one or two inflections on the long-wavelength side of the 275 nm band. Representative absorption spectra for the oxidized and reduced form are shown in Fig. 1. The large change in the absorption spectrum on reduction and the fact that aporubredoxin, formed by removing the iron (see above), shows no absorption bands at wavelengths longer than the normal protein band at 280 nm, is strong evidence that the chromophoric group contains the iron atom. The chromophore
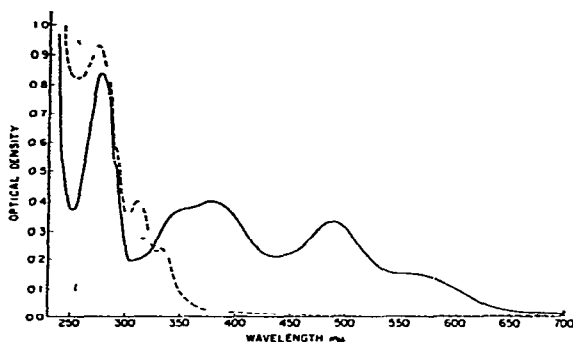

Fig. 1 Absorption spectra[80] of *Clostridium pasteurianum* rubredoxin, oxidized (———) and reduced (– – –) (Courtesy of the National Academy of Sciences, U S A)

responsible for the visible and near UV bands in the oxidized form also contributes to the 280 nm band, for the absorbance at 280 mμ is about twice that expected from the aromatic amino acid content, while an apoprotein derivative gives a 280 mμ extinction coefficient comparable to that expected from the aromatic amino acids[3].

The optical rotatory properties of rubredoxins from various sources are also nearly identical[1,55,79,104,117]. We shall discuss the circular dichroism principally, as it generally gives higher resolution. The CD curves for a representative rubredoxin in both the oxidized and reduced state are shown in Fig. 2. In the oxidized form, CD bands correspond closely to the absorption bands at 560, 490, 345 and 280 nm. A band at about 400 nm may be identifiable with the 380 nm absorption band. In addition, CD indicates the presence of electronic transitions at 630, 440, 328 and 224 nm which do not coincide with obvious features in absorption. In the reduced rubredoxins, CD bands at 336 and 317 nm correspond to absorption maxima. The region below 300 nm is complex, with sharp CD bands at 295, 287 and 258 nm, and a strong negative band at 224 nm, identical with or nearly identical with that in the oxidized form.

No CD data are available for aporubredoxin, but Lovenberg and Williams[81] reported the optical rotatory dispersion spectrum of an aporubredoxin. This spectrum is a typical protein ORD spectrum with no Cotton effects above 300 nm, weak inflections in the aromatic absorption region and a 233 nm trough whose
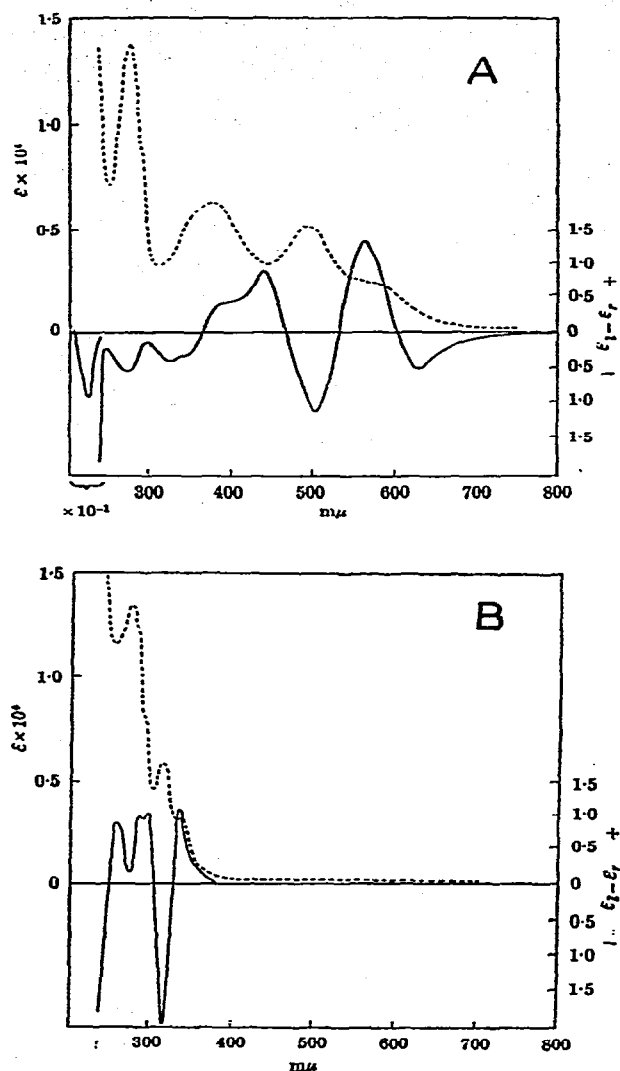
Fig. 2. Circular dichroism (———) and absorption (– – –) spectra of *Peptostreptococcus elsdeni* rubredoxin[1]: (A) oxidized, (B) reduced. The right-hand ordinate scale (CD) should be multiplied by a factor of 10 (Ref. 51). (Courtesy of MacMillan, Ltd.).

amplitude falls between that which was found for the oxidized and reduced rubredoxins.

The observed Cotton effects at wavelengths longer than 300 nm in both oxidized and reduced rubredoxins are attributable to the chromophore associated with the iron. Gillard *et al.*[55] have suggested that the transitions at 570 and 490 nm in oxidized rubredoxins may be magnetically-allowed transitions of the ligand–field ($d \rightarrow d$) type since they are especially prominent in the ORD and CD spectrum,

but weaker in absorption. They also suggest that the 390 nm band, with strong absorption and relatively weaker CD, may be an electrically-allowed charge-transfer (CT) band. However, the ratio of $\Delta\varepsilon$ to ε at the extrema is of the order of 10^{-3} for all three of these bands, ranging from about 0.5×10^{-3} for the 390 nm band to about 4×10^{-3} for the 560 nm band. This ratio, which is a rough approximation to Kuhn's anisotropy factor, is typically $\gtrsim 10^{-2}$ for magnetically-allowed and electrically-forbidden transitions[88]. The small value of this anisotropy factor, together with the large extinction coefficients, argues against the assignment of the 560 and 490 nm transitions as $d \rightarrow d$ transitions. It is more likely that the prominent visible and near UV absorption bands are of the charge-transfer type. Further, ligand $\rightarrow$ metal charge transfer bands would be expected to undergo a shift to higher energy (blue shift) on reduction of the metal, which would account for the disappearance of the visible absorption bands upon reduction.

The absorption bands at 630, 440 and 328 nm, which are apparent in CD but not in absorption may be magnetic dipole transitions, but even here one must remember that magnetic dipole character is not unique to $d \rightarrow d$ transitions. In particular, transitions involving non-bonding electrons on ligands could also contribute.

The assignment of bands below 300 nm is also uncertain. Several authors[1,117] have attributed the CD bands between 250 and 300 nm in oxidized and reduced rubredoxins to aromatic chromophores. Atherton et al.[1] suggest that the large changes in CD in the aromatic absorption region may indicate one or more aromatic groups near the site of reduction. However, the 280 nm band in absorption contains a substantial contribution from the iron-centered chromophore[3] and it is likely that the same chromophore may contribute substantially to the CD spectrum in this region.

The 224-nm CD band is presumably dominated by the peptide chromophores of the protein. However, some contributions from the iron-centered chromophore and from aromatic chromophores are also to be expected, and attempts to infer "helix content" from the amplitude of this Cotton effect are not likely to be successful. Even the observation of Atherton et al.[1] that reduction leaves the CD at 224 nm unchanged cannot be considered as strong evidence that oxidized and reduced rubredoxins have nearly identical conformations.

(iii) EPR

Rubredoxins in the oxidized state show an electron paramagnetic resonance signal at liquid nitrogen temperatures or below with a g value of about 4.3[1,2,79,104,117] and a second g value near 9[104,117]. These signals disappear upon reduction, and no new signal is observed even at temperatures as low[117] as 17 °K. Peterson and Coon[117] also showed that the loss of the EPR signal on reduction exactly parallels the loss of visible absorption at 490 mμ. The $g = 4.3$ and $g = 9$

signals of the oxidized state are characteristic of high spin ferric ions in a rhombic environment with either approximately tetrahedral[30] or octahedral[150] coordination.

The $g = 4.3$ signal of oxidized rubredoxins is unsymmetrical and generally consists of a narrow signal about 18 gauss wide, superimposed upon a much broader signal approximately 200 gauss in width. Double integration of this peak has led to estimates of spin content corresponding to 15%[2] and 36%[117] of the total iron present, assuming high-spin Fe^{III}. These low values are somewhat disturbing, but absolute calculations of spin concentration from EPR are difficult[14]. Sharper signals and better results may be obtainable at lower temperatures.

Bachmayer et al.[2] observed that at pH 10, the broad and sharp components of the EPR signal present at neutral pH, merge into a single nearly symmetrical component of intermediate width, without any change in total intensity. They interpreted this change as indicating a modification of the two non-cysteine ligands which they believed to be present. It is possible that the effect of high pH on the $g = 4.3$ resonance is due to the ionization of a nearby lysyl or tyrosyl group which is close enough to perturb the EPR signal, but is not actually a ligand, or the change could be due to a more general pH-induced conformational change.

(iv) X-ray diffraction

Jensen and co-workers[61] have recently reported results of an X-ray crystallographic study at 2.5 Å resolution of the rubredoxin from Clostridium pasteurianum. Unfortunately, the amino acid sequence for this protein has not been determined, so that a detailed interpretation of the Fourier map has not been carried out. Nevertheless, they can see the iron atom and four surrounding cysteine sulfurs very clearly. Furthermore, the S–Fe–S angles are all within 13° of the tetrahedral value of 109.5°. Since they estimate the r.m s. error for bond angles at this stage to be about 8°, their conclusion is that the coordination of Fe by sulfurs is essentially tetrahedral. These workers do not mention the presence of any other ligands, and if the sulfurs are indeed arranged in a tetrahedron, the presence of other ligands is improbable.

(v) Discussion

There are still many gaps in our knowledge of these simplest iron–sulfur proteins, the rubredoxins. However, approximately tetrahedral coordination of iron by four cysteine sulfurs appears to be the most likely structure. This is largely based on the X-ray work of Herriott et al.[61], but is consistent with all the other data. Such coordination would be expected to leave the iron in a high-spin state. Studies[128] of Fe^{II} ions occupying cation vacancies in ZnS in which the iron is tetrahedrally coordinated by sulfide ions have been carried out. The absorption spectra of these systems show $d \to d$ transitions in the infrared in the 3-μ wave-

length region. Some absorption bands also appeared in the visible, but all but a few very weak bands could be assigned to traces of Co^{2+} present also in the crystals. Such spectra are consistent with high-spin Fe^{II} ions, which have only one spin-allowed $d \rightarrow d$ transition, $^5E \rightarrow {}^5T_2$ in tetrahedral symmetry. All higher-energy $d \rightarrow d$ transitions are spin-forbidden, involving singlet or triplet upper states.

Slack *et al.*'s ligand-field analysis[128] of the spectrum yielded a value of -3400 for $10Dq$, the splitting between the e and t_2 d orbitals (the minus sign arises from the inversion of the e and t_2 orbitals in tetrahedral coordination). No comparable studies are available for Fe^{III} surrounded by four S ligands. However*, one can make a rough estimate that $10Dq$ for Fe^{III} should be about -4800 cm^{-1} in ZnS. Both Fe^{II} and Fe^{III} should be high spin when tetrahedrally coordinated by four sulfurs. High-spin Fe^{III}, with a $^6A_1$ ground state in tetrahedral symmetry has no spin-allowed $d \rightarrow d$ transitions. Thus, neglecting spin-forbidden transitions, one cannot assign the observed transitions in the visible spectrum of oxidized rubredoxin to $d \rightarrow d$ transitions. This is consistent with the large intensity of these bands and the low value of the $\Delta\varepsilon/\varepsilon$ ratio.

A ligand $\rightarrow$ metal charge transfer assignment for the visible absorption bands is quite plausible, however. Calculations[153] using Jørgensen's optical electronegativity parameters[69,77] predict that the lowest energy charge transfer transition for an Fe^{III} ion with four sulfur ligands should occur between 600 and 700 nm, while in an Fe^{II} complex, the transition would be blue shifted to about 260 nm. These predictions agree as well as could be expected with the observations of the absorption bands at 560 nm in the oxidized form and at 330 nm in the reduced form of rubredoxin.

As we have seen, the EPR spectrum of the oxidized rubredoxin is consistent with high-spin Fe^{III} in distorted tetrahedral symmetry, though it would also be consistent with distorted octahedral symmetry. It should be pointed out, however, that this model also predicts that the reduced form is paramagnetic, and might show an EPR spectrum. No EPR signals have been observed for reduced rubredoxin, but it is possible that one must go to lower temperatures than 17 °K, apparently the lowest temperature at which such signals have been sought[117]. In any event, magnetic susceptibility studies need to be carried out on both oxidized and reduced rubredoxins. These should unambiguously determine the spin states of the iron. Mössbauer spectroscopy has not been applied to these systems, either, and it could provide useful information on rubredoxin, as well as helping in the interpretation of Mössbauer data on more complex iron–sulfur proteins.

---

* This is based on data compiled by Figgis[48]. The relative values of 10 Dq for Fe^{III} and Fe^{II} can be estimated from Table 9.5, p 244 The ratio should be about 14/10, leading to a value of 10 Dq $\sim$ -4800 cm^{-1} for Fe^{III} in a tetrahedral site in ZnS.

C. 2Fe–2S* PROTEINS

(1) Chemistry

Iron–sulfur proteins of this class contain two atoms each of iron and acid-labile sulfur per molecule[85]. Reported molecular weights are generally about 12,000, but in a few cases substantially higher values have been reported. These proteins are found in animals (e g , in adrenal glands), plants (e.g., spinach), bacteria (e g., Pseudomonas putida), and represent the simplest iron-acid labile sulfur species

Amino acid sequences of four green-plant ferredoxins have been reported[18,71,91,131]. The positions of five cysteines are identical among these four proteins, but Scenedesmus ferredoxin contains an extra cysteine residue. Two cysteines occur in the sequence –cys–X–Y–cys– in each case, while the others appear isolated. By analogy to the rubredoxins, it appears likely that the two closely spaced cysteines are bound to iron. Some or all of the others may also be involved in the active center.

Massey[89] and others[72] have reported the evolution of H_2S, measured by the "methylene blue" method[50] upon acidification of succinic dehydrogenase and various ferredoxins. H_2S is also lost from these proteins on long standing at room temperature and neutral pH. This is unusual for proteins because under these conditions no H_2S is evolved from cysteine, cystine or methionine residues. There has been a controversy in the literature concerning the origin of the evolved H_2S. For clostridial ferredoxin (see Section E) the release of H_2S was postulated to occur through a β-elimination from the cysteine residues[7,52], although now[8,83] it is generally agreed that this is not the case. This subject has been thoroughly discussed by Malkin and Rabinowitz[85]. Elemental sulfur analyses in conjunction with amino acid analyses in putidaredoxin, a bacterial 2Fe–2S* protein, and apoputidaredoxin[140] also suggest that the acid-labile sulfur does not come from cysteine or methionine.

Iron is released from these proteins by adding acid or a mercurial. This suggests that the iron is bound to the protein via sulfur ligands. However, the iron release might also be effected by an unfolding of the peptide chains.

The iron is usually determined by colorimetric methods[8,89,143,146]. Attempts to determine the valence of the released iron by using various chelating agents should be interpreted with caution because the valence state may change during analysis[113] due to reaction with the reagents, with evolving H_2S in the presence of air, or with groups on the protein, especially –SH or –SS–.

One can easily obtain the apoprotein (free of iron and acid-labile sulfur) and reconstitute the active protein with salts of iron and sulfide. We give a short description of the procedures in use; most of them were developed first for the nFe–nS* proteins but are probably applicable to all iron–sulfur proteins.

Lovenberg et al.[82] used a mercurial to release the iron and sulfide from clostridial ferredoxin. Malkin and Rabinowitz[83] isolated the apoprotein from the reaction mixture by column chromatography with DEAE-cellulose or Sephadex G-25. Bayer et al.[8] treated the same protein with α,α'-bipyridyl. This treatment slowly removes the iron from the protein and releases H_2S.

The active protein can be reconstituted by adding to the apoprotein an excess of 2-mercaptoethanol, an iron salt ($FeCl_3$), and Na_2S. Bayer et al.[8] have substituted cysteamine or dithiothreitol for 2-mercaptoethanol and elemental sulfur for Na_2S. The addition of the sulfhydryl reagent is required for high-yield reconstitution as in the case of the rubredoxins.

An alternative method for the release of iron and sulfide, which has been used with putidaredoxin[141,142], is an anaerobic precipitation of the apoprotein with 20% trichloroacetic acid (TCA). The apoprotein is washed twice with 20% TCA to remove any remaining iron or sulfide. The native protein can be reconstituted by adding an excess of iron salt and Na_2S. Under these conditions no 2-mercaptoethanol is required; it can be added later for manipulations in the presence of air. Hong and Rabinowitz[63] reported a similar aerobic TCA precipitation of clostridial ferredoxin with and without 2-mercaptoethanol; for reconstitution 2-mercaptoethanol is needed. Therefore, it seems that the role of the sulfhydryl reagent is to reduce sulfur ligands on the protein which have been oxidized during the isolation of the apoprotein.

Iron–sulfur proteins serve as carriers in electron transport in biological systems. Their redox potentials (E_m at pH 7) vary, e g., -430 mV for spinach ferredoxin[133], -367 mV for adrenodoxin[46], -235 mV for putidaredoxin and -241 mV for Se-putidaredoxin[152]. The values for adrenodoxin and putidaredoxin are corrected from those previously reported[72]. Electrochemical potential measurements have sometimes been in error due to electrode poisoning and interfering species in solution. The putidaredoxin measurements were performed spectrophotometrically in the presence of any of a series of reduced quinones at equilibrium with the protein[152].

Only one electron is taken up by putidaredoxin and adrenodoxin on reduction by dithionite[13,107,142]. These studies have shown that the uptake of one electron per molecule (2 irons) produced a maximal EPR signal (see below) and bleaching of the visible spectrum. Kimura[72] reported a value of two electrons per mole of adrenodoxin.

(ii) Optical spectroscopy

The optical absorption spectra of 2Fe–2S* proteins from a number of species have been reported[37,114,133]. Although there are slight variations in location of spectral features and in extinction coefficients, the spectra are sufficiently similar that there is little doubt that one is dealing with a single well-defined chromophore

in all of these systems. Fig. 3 shows the absorption spectra of putidaredoxin in the oxidized and reduced (by dithionite) forms[153]. There are distinct maxima at 455, 412, 328 and 276 nm and a weak shoulder at about 560 nm in the oxidized form. Upon reduction, the spectrum is greatly altered, showing maxima at 540 and 274 nm and inflections at about 460, 390, 355 and 310 nm. Considerably better resolution is attainable at liquid nitrogen temperatures[114,153]. Wilson[151] has reported spectra in the red and near IR region at liquid nitrogen temperatures for spinach ferredoxin and adrenodoxin.
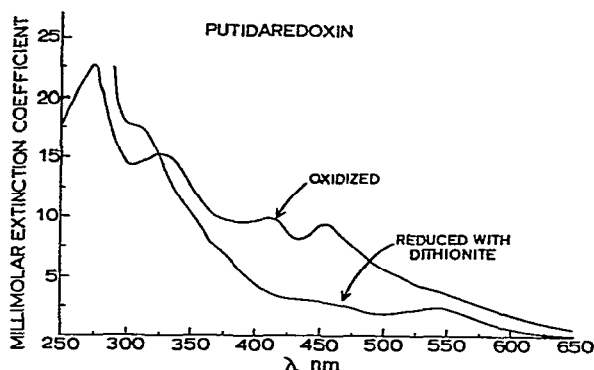

Fig 3   Absorption spectrum of putidaredoxin[153].

Woody et al.[153] have also measured the absorption spectrum of putidaredoxin in which the labile sulfurs have been replaced by selenium[143]. In this derivative, the shape of the absorption spectrum is very similar, although the bands tend to be somewhat broader. The most striking difference is a more or less uniform displacement of all of the bands to longer wavelengths by about 10–30 nm. Comparable shifts are seen in the absorption spectrum of the reduced Se derivative.

The optical rotatory properties of several green-plant ferredoxins, adrenodoxin and putidaredoxin have been studied[51,114,145,153]. The CD spectrum of selenium substituted putidaredoxin has also been measured[153]. These seemingly diverse proteins show strikingly similar CD and ORD spectra. The CD spectra of spinach ferredoxin and adrenodoxin[114] and of putidaredoxin and its selenium analogue[153] have been analyzed into components, assuming Gaussian bandshapes, and rotational strengths have been calculated. There is in general a one-to-one correspondence in CD bands among these four proteins, allowing for a red shift of 10–30 nm in the Se protein, and approximate agreement in the rotational strengths.

Palmer et al.[114] point out that the ratio of $\Delta\varepsilon/\varepsilon$ over the visible region is of the order of 10^{-3}–10^{-4}, and that this ratio is not sufficiently large to clearly implicate magnetically-allowed transitions (e.g. $d \rightarrow d$ transitions).

The observation of a red shift on selenium substitution is consistent with a

ligand → metal charge transfer assignment for the visible absorption band. Further, the position of these bands strongly suggests that the iron is in the *ferric* state in the oxidized form, not in the ferrous (see discussion of rubredoxins, Section B, *v*).

(iii) EPR, ENDOR and magnetic susceptibility

When reduced, all 2Fe–2S* proteins exhibit at sufficiently low temperatures a characteristic EPR signal with $g_{\parallel}(g_z) = 2\ 01$ and one or two high-field g values ($g_{\perp} = 1.94$, axial symmetry, or $g_x = 1\ 89$ and $g_y = 1.94$, rhombic symmetry). Beinert and Sands[15] first observed this signal, at temperatures below 150 °K, in mitochondrial preparations and proteins after reduction with dithionite or substrates. This signal has also been seen in samples of source material of iron–sulfur proteins, e g., liver, heart or mitochondria[16]. EPR spectroscopy has been used subsequently[126] to monitor the purification of iron–sulfur proteins The origin of the $g = 1.94$ signal was not known at first although a transition metal was considered very likely Shethna *et al* [125] showed that the signal was due to iron by comparing the signals of protein isolated from a nitrogen fixing bacterium, *Azotobacter vinelandii*, grown in media with natural abundance iron (^{56}Fe, nuclear spin $I = 0$) to that with 65% enriched ^{57}Fe ($I = \frac{1}{2}$). The protein from the ^{57}Fe medium showed a broadened signal compared to that from the ^{56}Fe medium

Now with reconstitution procedures (see Section C, *i*) one can put ^{57}Fe (of high enrichment, $\geq 90\%$) in the pure proteins. Thus, expensive ^{57}Fe growth experiments can be avoided and also ^{57}Fe-enriched samples of plant and animal proteins are available for studies. However, not all proteins are suitable for this EPR approach, e.g., native spinach ferredoxin shows a rather broad EPR spectrum[114] at *ca.* 40 °K and isotopic substitutions cause only marginal additional broadening.

With EPR studies on two 2Fe–S* proteins, putidaredoxin and adrenodoxin, it was possible to determine the *number* of iron atoms that interact with the unpaired electron[13,107,142]. Fig. 4 shows the EPR spectra of native, ^{56}Fe reconstituted and ^{57}Fe reconstituted putidaredoxin. The spectra of native and ^{56}Fe reconstituted protein are superimposed and indistinguishable illustrating that the reconstitution procedure (anaerobic TCA precipitation) itself does not alter the signal shape The splitting or broadening of the ^{57}Fe spectrum depends on three variables, if we assume a predominantly isotropic hyperfine interaction, *viz.*, the enrichment in isotope (^{57}Fe) of non-zero nuclear spin, the effective local field contribution or hyperfine coupling constant of each atom, and the number of ^{57}Fe atoms interacting with a single unpaired electron. If the enrichment is known, one can calculate spectra that result from various hyperfine splittings and numbers of ^{57}Fe atoms. In favorable cases, the comparison of the trial spectra with the observed spectrum reveals the values of the variables. Fig. 5 shows a superposition of a ^{57}Fe-substituted putidaredoxin spectrum and a computer simulated one. This

simulation was based on the EPR signal of the native (^{56}Fe) protein and the interaction of the unpaired electron with *two* iron-57 nuclei. The ^{57}Fe enrichment was assumed to be 94% and the hyperfine splitting 14 gauss. Similar results were obtained by Beinert and Orme-Johnson[13] with ^{56}Fe- and ^{57}Fe-adrenodoxin
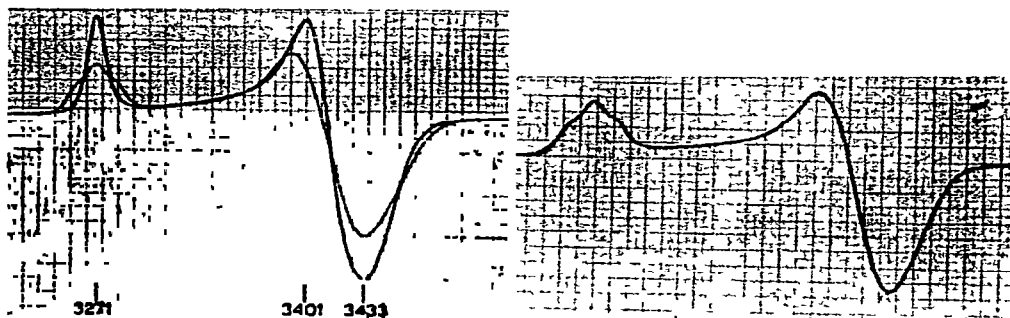

Fig 4 EPR spectra of reduced putidaredoxin[142] The spectra of the native protein and after reconstitution with ^{56}Fe are superimposed and indistinguishable The broadened spectrum is the putidaredoxin reconstituted with ^{57}Fe at 90 7% enrichment Line amplitudes are adjusted so the three curves represent equal quantities of unpaired electrons (Courtesy of the National Academy of Sciences, U S A)

Fig 5 Computer simulation of EPR spectrum of ^{57}Fe-substituted reduced putidaredoxin, based on the spectrum of the reduced native protein and interaction of the unpaired electron with two iron nuclei[142] The spectrum of the reduced protein, in which iron has been exchanged with ^{57}Fe, is superimposed on the computed spectrum (Courtesy of the National Academy of Sciences, U S A).

As mentioned already, a unique feature of these iron–sulfur proteins is the presence of acid-labile sulfur. It was suggested that sulfur may also be associated with the characteristic $g = 1.94$ signal. This is indeed the case as shown by Hollocher et al.[62] and DerVartanian et al.[41]. The first group used *Azotobacter vinelandii* grown in ^{33}S-enriched media and observed the broadened EPR signal in the whole cells. The signal broadens indicating coupling of the electron spin with one or more sulfur nuclei (^{33}S has a nuclear spin $I = \frac{3}{2}$ whereas ^{32}S has $I = 0$) The second group observed the signal in purified proteins from *Azotobacter* and *Pseudomonas putida* grown on ^{33}S. Later, Tsibris et al.[142] showed that at least part of this sulfur is of the acid-labile type by reconstituting putidaredoxin from ^{32}S grown cells with ^{33}S-sulfide (48 5% enriched in ^{33}S) and observing a broadened EPR spectrum. A quantitative evaluation of the participating sulfur atoms is complicated by two factors[108]. First, the $\frac{3}{2}$ nuclear spin of ^{33}S leads to seven hyperfine lines for two interacting nuclei. Second, ^{33}S enrichment higher than 50% is extremely rare; the use of only 50% enriched ^{33}S-sulfide complicates the analysis because on the average one half of the protein molecules would contain only one ^{33}S atom. Thus the expected hyperfine pattern contains contributions from molecules with no ^{33}S (25%, one line), one ^{33}S (50%, four lines) and two ^{33}S atoms (25%, seven lines). Overall, the expected pattern would contain 11 hyperfine lines; only a very

large value of the hyperfine coupling constant would allow the unraveling of the situation.

Orme-Johnson et al.[108] sought an alternative method in solving this problem. They used the selenium analogues of putidaredoxin and adrenodoxin. Selenium putidaredoxin, a biologically active protein, was prepared by Tsibris et al.[143] by reconstituting the apoprotein with $(NH_4)_2Se$ rather than Na_2S The isotopes ^{77}Se $(I = \frac{1}{2})$ and ^{80}Se $(I = 0)$ are available in ca. 90% enrichment. Fig. 6 shows the
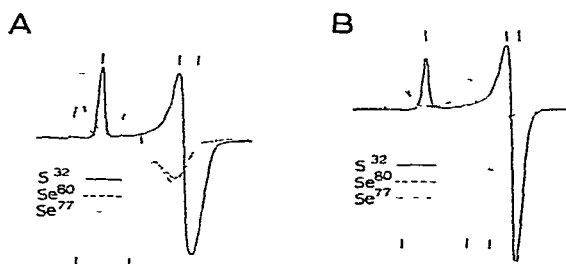
Fig. 6 (A) Superposition of EPR spectrum[108] of putidaredoxin in natural form (^{32}S) and with the labile sulfur substituted by Se isotopes Intensities are matched within $\pm 5\%$ to represent equal amounts of unpaired electrons Upper field markers correspond to ^{32}S curve, the lower ones to Se curves They indicate from left to right (upper) 3262, 3391 and 3423 gauss, and (lower) 3227 and 3315 gauss at 9,221 7 MHz, (B) superposition of EPR spectra[108] of iron–sulfur protein from pig adrenals, in natural form and with Se substitution, as in Fig 6a. Upper markers 3259, 3394, 3476 gauss, lower markers, 3222, 3332, and 3370 gauss, all at 9,213 4 MHz (Courtesy of the National Academy of Sciences, U S A)

spectra of ^{32}S, ^{80}Se, ^{77}Se-substituted putidaredoxin and adrenodoxin. It should be noted that the EPR signal of Se–putidaredoxin has lost the axial symmetry seen in the native protein (three g values can be distinguished) whereas Se–adrenodoxin has retained it. A computer simulation of the spectra, as in the case of ^{57}Fe-substituted proteins, shows that at the enrichment of 87% ^{77}Se the observed hyperfine pattern (10 gauss/Se) can only be explained as resulting from the interaction of two Se nuclei with one unpaired electron assuming that the two Se nuclei produce the same splitting. This strongly suggests that in natural putidaredoxin and adrenodoxin the paramagnetic center includes both iron atoms and both acid-labile sulfur atoms. This does not, of course, exclude contributions from other ligands from the protein backbone groups, solvent molecules and other unidentified small molecules.

Tsai et al.[139] have shown recently that sulfur atoms, other than the acid-labile ones, also participate in the paramagnetic center of putidaredoxin. Fig. 7 shows a superposition of the EPR spectra of isotopically substituted putidaredoxins. A quantitative evaluation of the total number of sulfur atoms in the active center is in progress.

A titration of putidaredoxin[142] and adrenodoxin[13] by the solid-diluted dithionite method of Orme-Johnson and Beinert shows that one electron is ac-
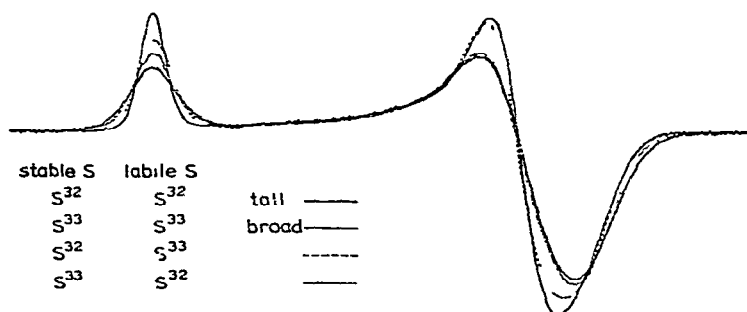
Fig 7. Superposition of EPR spectra of putidaredoxins (reduced) Solid curves refer to unre-constituted proteins grown on ^{32}S (tall) and ^{33}S (broad) media The broken curves correspond to reconstituted samples "Stable sulfur" (i e , sulfur in amino acid side chains) is determined by the growth medium, "acid-labile" sulfur by the isotopic form of Na_2S used in reconstitution. All curves represent equal numbers of unpaired spins[139].

cepted per molecule of protein by the criteria of EPR spectroscopy and the bleaching of the visible spectrum. Double integration of the signals of maximally reduced proteins indicated that one electron per molecule of protein was quantitatively represented in the EPR spectrum.

Sands[122] has reported recently the first successful ENDOR experiments with putidaredoxin and other iron–sulfur proteins. In these experiments, performed at ca 20 °K, an EPR transition (e.g., $g = 2.01$) is nearly "saturated" by increased microwave power and therefore the signal diminishes; a nuclear transition is then induced by the absorption of radio-frequency radiation If the unpaired electron is coupled to the nucleus that undergoes the transition the difference in the electronic populations will change and therefore the amplitude of the EPR signal will be altered. An ENDOR spectrum shows the amplitude of the EPR signal as a function of the applied radio-frequency radiation. Thus ENDOR combines the high sensitivity of EPR with the high resolution of NMR spectroscopy.

Analysis of the ENDOR spectra reveals a number of parameters like the A (hyperfine coupling constant) tensor, which in combination with the g tensor from EPR make feasible the computer simulation of Mössbauer (determination of the electric field gradient tensor) and ENDOR spectra and the comparison with models of the paramagnetic center.

Initial ENDOR experiments[123] on putidaredoxin indicate that both iron atoms, having very similar hyperfine coupling constants, are in identical sites in the reduced form, in agreement with previous Mössbauer data[31]. Preliminary ENDOR studies also indicate that some protons are "coupled" to the paramagnetic center. If the protein is dissolved in D_2O some protons are lost from the ENDOR spectrum. Further studies at pH 8.3 and 6.5 are being conducted to clarify the participation of protons in the active center of these iron–sulfur proteins.

ENDOR studies of spinach ferredoxin[122] indicate that the EPR line-broadening in the unsubstituted enzyme is due to interaction of nuclei other than iron

with the electron. This presumably accounts for the failure of EPR isotopic substitution experiments[111] to show clear evidence of hyperfine splitting due to ^{57}Fe.

Magnetic susceptibility studies of oxidized and reduced spinach and parsley ferredoxins have been reported by Moss et al.[101] and have also been carried out by Ehrenberg (quoted by Thornley et al.[138]) on spinach ferredoxin. Ehrenberg reportedly found $\chi = 1015 \times 10^{-6}$ e.m.u. per iron atom in the oxidized state and $\chi = 2285 \times 10^{-6}$ e.m.u. per iron in the reduced state of spinach ferredoxin at room temperature. Moss et al.[101] found that oxidized spinach ferredoxin has a temperature independent susceptibility almost identical to that of a buffer blank, indicating no unpaired electrons and little or no temperature independent paramagnetism. When reduced, the spinach ferredoxin shows Curie law behavior from 1.4–201 °K with a slope of χ_V (volume magnetic susceptibility) vs. T corresponding to a spin $\frac{1}{2}$ system. Oxidized parsley ferredoxin behaves similarly, except that a small paramagnetism is indicated, corresponding to less than 15% of that expected for a single unpaired electron. This is attributed to a trace amount of paramagnetic impurity. As the authors point out this residual paramagnetism can be accounted for if only 1% of the ferredoxin molecules were denatured and the iron were in the high spin $S = 5/2$ state.

(iv) Mossbauer spectroscopy

Information from Mössbauer measurements complements knowledge on the protein active center obtained by EPR, ENDOR, chemical and other techniques. Ideally, Mössbauer spectroscopy can give an insight into the immediate geometry and electronic configuration of the iron.

Mossbauer spectra of 2Fe–2S* proteins[10,31,65,67,100] obtained in the oxidized state consist of a pure quadrupole doublet with small linewidths (Fig. 8). From this, one concludes that both iron atoms are in equivalent sites. In order to explain the diamagnetism we must assume that the two irons interact to form an antiferromagnetic pair, or are low-spin Fe^{II}. The isomer shift (ca. 0.46 mm/sec relative to sodium nitroprusside or 0.2 mm/sec relative to iron metal) is independent of temperature (except for a second-order Doppler effect). The quadrupole splitting, ca. 0.6 mm/sec, shows[31] a slight decrease at temperatures above 200 °K.

When a strong external magnetic field (30 Kgauss) is applied, the Mössbauer spectrum changes[67], Fig. 9, as expected from a diamagnetic compound. No effect due to an internal magnetic field was observed. From these measurements on Euglena ferredoxin it is concluded that the principal component of the electric field gradient has a positive sign.

Upon reduction, enzymatically or with dithionite, the spectra change drastically[40], Fig. 10. It should be noted that a small external field (ca. 20 gauss) can decouple the nuclear and electron spins. The addition of one electron per molecule
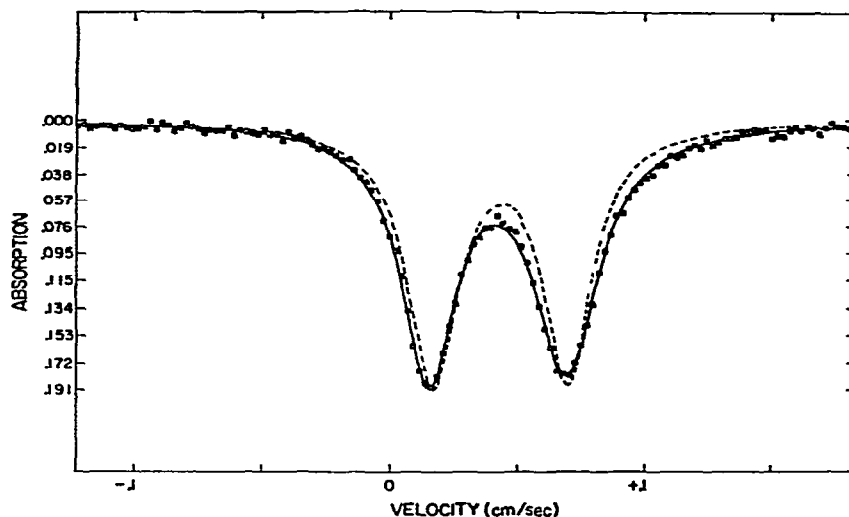
Fig. 8. Mossbauer spectrum of oxidized putidaredoxin at 100 °K[31]. Tne solid line is a computer-fit to the data for a sample before treatment with dithioerythritol (DTE) The dotted line represents the computer fit to the spectrum of the sample after treatment with DTE. Zero Doppler shift corresponds to the center of the sodium nitroprusside spectrum (Courtesy of the National Academy of Sciences, U S A.)
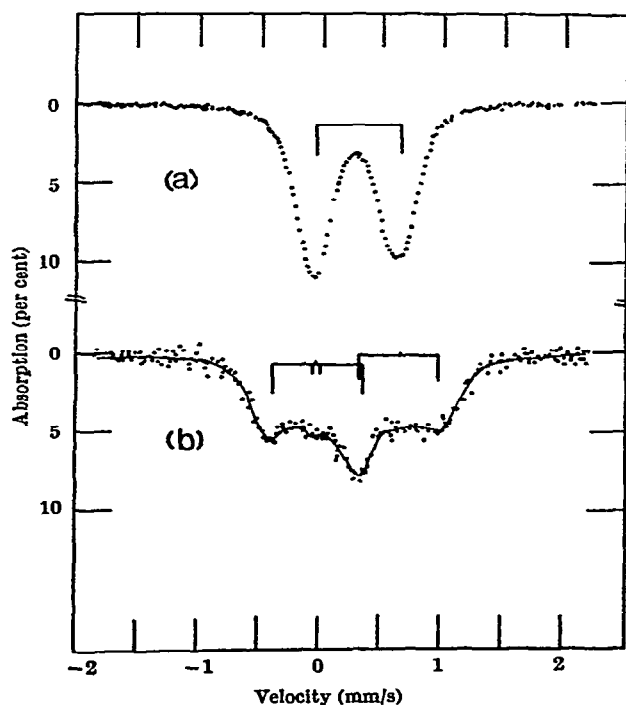

Fig. 9. Mössbauer spectra[65] of ^{57}Fe *Euglena* ferredoxin at 4 2 °K. (a) No applied field, (b) 30 gauss applied field perpendicular to gamma ray beam (Courtesy of MacMillan, Ltd)
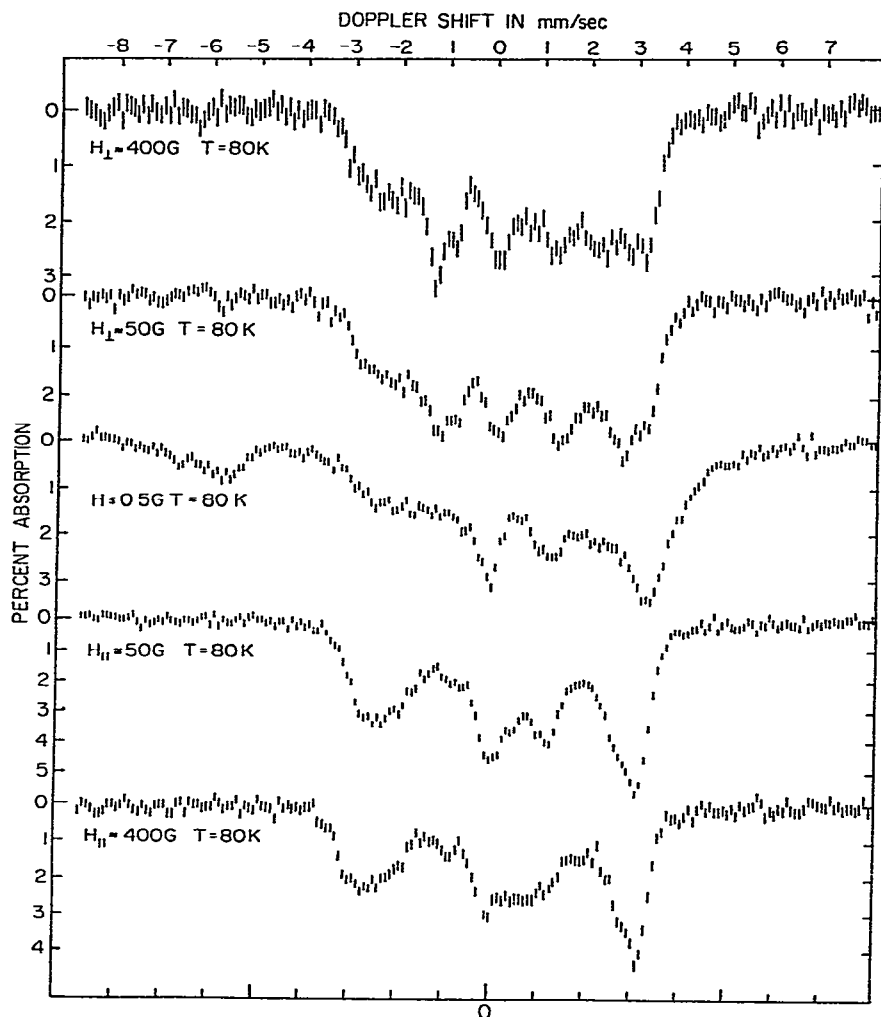
Fig 10 Móssbauer spectra of ^{57}Fe putidaredoxin (reduced form) showing the effect of small magnetic fields[40].

of putidaredoxin completely erases the oxidized spectrum, a fact confirmed by EPR titration[142]. The spectra in the reduced state are temperature-dependent and quite complex. The marked temperature dependence, along with the broadness of the lines, indicates electron-spin relaxation effects at higher temperatures. The large splitting at low temperatures is attributed to a magnetic hyperfine interaction; an effective field of ca. 140 Kgauss at the iron nucleus can be calculated. At temperatures ca. 200 °K the magnetic hyperfine interaction partially averages out in the zero-field spectra. The remaining structure is still relatively complex and must be due mainly to quadrupole interaction. At 262 °K most of the putidaredoxin spectrum[31] intensity has coalesced into a broad central line. Thus, averaged over a

nuclear lifetime the spectra of the two iron sites again appear identical with the additional electron being shared between the two irons. This conclusion is confirmed by recent ENDOR studies [cf. Section C (iii)].

In spinach ferredoxin (originally designated as PPNR) reduction by dithionite seemed to reduce only one of the two iron atoms[65,100]. However, further studies[68] indicate that the irons in fact are equivalent in reduced ferredoxin.

(v) Nuclear magnetic resonance (NMR)

Mildvan et al.[95] measured the nuclear magnetic spin–lattice and spin–spin relaxation rates of water protons in solutions of adrenodoxin and spinach ferredoxin. They concluded that the solvent protons do not gain access to the coordination sphere of iron when the above proteins are in the oxidized state. Upon reduction with dithionite there occurs a slow exchange of solvent protons with those of the coordination sphere in adrenodoxin but not ferredoxin. Thus, they conclude that reduction may increase the accessibility of protons to the paramagnetic center of adrenodoxin.

(vi) Discussion

Because the techniques discussed have not all been brought to bear on each of the proteins in the 2Fe–2S* class, generalizations are hazardous. Nevertheless, the similarities in the optical, CD, EPR and Mossbauer spectra of these systems suggest a very close similarity among them, notwithstanding the fact that two subclasses (the green plant ferredoxins vs. components of hydroxylases) can be distinguished. Thus, we envision all of these systems as involving an active center containing the 2 Fe atoms and the 2 labile sulfurs in close proximity. In the oxidized state, these systems are diamagnetic, and they take up a single electron (within the accessible range of reductants in aqueous media) to form a doublet $S = 1/2$ system. The optical spectra indicate that the iron is Fe^{III} in the oxidized form, but it is not certain whether it is in a high- or low-spin state, nor whether the coordination is approximately octahedral, tetrahedral, or has some other less ordinary stereochemistry.

Several models have been proposed for these 2Fe–2S* proteins. Earlier suggestions have been reviewed by Beinert[12]. The principal object of these models has been to explain the unusual EPR characteristics, which are nearly unprecedented in well characterized Fe complexes. The unique feature of the iron–sulfur protein EPR spectra with $g = 1.94$ signals is that the average g-value is less than 2, the free-electron value[12,142]. Beinert et al.[17] reported that pentacyanonitrosylferrate (I) at low temperatures in aqueous media shows an EPR signal with $g_\perp = 2.00$ and $g_\parallel = 1.92$. Though the average g-value is indeed less than 2.00 for this system, $g_\parallel$ is less than $g_\perp$, in contrast to the iron–sulfur protein case. Brintzinger et al.[27]

have found another example in bis-(hexamethylbenzene)Fe^I which has g values of 1.86, 1.99 and 2 08. Interesting though these models may be, the ligands are distinctly non-physiological.

Blumberg and Peisach[22] proposed that the $g = 1.94$ signals observed in iron–sulfur flavoproteins could arise from coupling of a diamagnetic ion, such as low-spin Fe^{2+} or Co^{3+}, with a free-radical such as a flavin, sulfur or aromatic side-chain radical. (At the time, $g = 1.94$ signals had not been observed in ferredoxins and other non-flavin proteins.) They demonstrated EPR signals with g-values less than 2 in several systems containing Fe^{2+} and Co^{3+} and benzoquinone, flavin or N,N-dimethyl-p-phenylenediamine. None of these complexes are well-characterized however, and the details of Blumberg and Peisach's theoretical work have not been published.

A more concrete model has been proposed by Brintzinger et al.[28]. This model envisions the iron-sulfur center as two iron-centered tetrahedra joined at an edge. The labile sulfurs form the bridging ligands, and two cysteine R–S groups are bound to each iron to complete the tetrahedra. It was assumed that each iron in the oxidized state is low spin Fe^{III}, and the absence of an EPR spectrum was attributed to exchange coupling leading to an $S = 0$ ground state, or to extreme line broadening. In the reduced form, it was assumed that one iron becomes Fe^{II}, the other remains Fe^{III}, both in low spin states, and that the EPR signal arises from Fe^{III}. The tetrahedral coordination was assumed in order to account for two g-values below 2 within the limits of crystal-field theory. To reproduce the exact departures of the g-values from $g = 2$, a very large crystal field splitting had to be assumed (20–30×10^3 cm^{-1}). As has been mentioned in discussing rubredoxin, such large ligand field splittings are highly unlikely for iron complexes with sulfur ligands in tetrahedral coordination. Sands[123] has subsequently considered the effect of introducing the spin–orbit coupling due to sulfur ligands. This reduces the necessary splitting to more reasonable values of the order of $10,000$ cm^{-1}, but this is still about twice as large as one might expect for such coordination. There are no known examples of low-spin tetrahedral complexes of first row transition metal ions[34]. In light of the Mössbauer, EPR and ENDOR results indicating equivalence and proximity of the two irons, attempts to treat the system as a one-iron problem may well lead to erroneous conclusions.

Gibson et al,[54] have proposed a model which does not appear to be inconsistent with any of the observations made thus far. They assume that the center contains two high-spin Fe^{III} irons in the oxidized form, but that these are anti-ferromagnetically coupled to form a singlet state ($S = 0$), consistent with the observed diamagnetism and lack of EPR signals in the oxidized form. In the reduced state, one has a high-spin Fe^{III} ($S = 5/2$) antiferromagnetically coupled to a high-spin Fe^{II} ($S = 2$) to yield a ground-state of $S = 1/2$. The effective g-values for such an antiferromagnetically coupled system can be calculated, neglecting spin–orbit coupling contributions at ligand centers. The observed g-values for

spinach ferredoxin can be reproduced with a distorted tetrahedral field having an average ligand field splitting of about 4000–5000 cm^{-1}.

Thornley et al.[138] showed that assuming the hyperfine coupling constant for a single ^{57}Fe nucleus is 10 gauss, the model of Gibson et al.[54] would lead to an overall hyperfine splitting of 37 gauss for the ground state doublet. This is to be compared with the observed values of 22 gauss for the overall splitting in the Azotobacter protein[125], less than 22 gauss in spinach ferredoxin[109], and 28 gauss in putidaredoxin[142]. The exact value to be assumed for the coupling constant for a single iron center in these systems is not known with any precision, so that the significance of the variation of experimental splittings among the three systems and the deviation from that predicted by Thornley et al. is questionable.

Thornley et al.[138] also considered Ehrenberg's magnetic susceptibility data in the light of the model of Gibson et al.[54]. The apparent weak paramagnetism of the oxidized state observed by Ehrenberg could be explained as arising from the thermal population of $S = 1$, $S = 2$, etc. states at room temperature, implying an antiferromagnetic coupling, J, of the order of -200 to -400 cm^{-1}, which are plausible values comparable to that observed by Bleaney and Bowers[20] for copper acetate monohydrate (-300 cm^{-1}). The more complete study of Moss et al.[101] indicates that oxidized spinach ferredoxin is essentially diamagnetic up to 210 °K, requiring a substantial anti-ferromagnetic coupling From their data, Moss et al. conclude that the coupling must be appreciably greater than thermal energies corresponding to 60 °K ($\sim$40 cm^{-1}). Thus the susceptibility data appear to be consistent with such a model, but until accurate data over the temperature interval from 200 °K to room temperature can be shown to fit such an anti-ferromagnetic coupling model, they cannot be said to directly support it.

It has also been pointed out by both Brintzinger et al.[28] (quoting a suggestion of R. J. P. Williams) and by Gibson et al.[54] that a highly covalent distorted octahedral model for the iron coordination cannot be ruled out, since the $4d^5$ complex Ru(NH$_3$)$_6$$^{3+}$ and several complexes of Ir^{III}d^5 give EPR signals with two g-values below 2.

Tetrahedral coordination of the iron in these 2Fe–2S* complexes is perhaps made more attractive by the strong evidence that such coordination is present in rubredoxins. Octahedral coordination would require that other ligands than sulfur be involved. For example, spinach ferredoxin contains only 5 cysteines and no methionines. Adrenodoxin contains 4 cysteines and 1 methionine. Counting the two labile sulfides 7 S ligands are available in each case. The total number of ligands required for octahedral coordination depends upon how many ligands act as bridges between the two irons. If the octahedra are independent, 12 ligands would be required. If the octahedra shared corners, edges or faces, 11, 10 and 9 ligands, respectively, would be involved. There is no evidence for or against the presence of other ligand groups at present. Further ENDOR experiments should be able to decide whether or not nitrogen or oxygen ligands are present.

D. 4Fe–4S* PROTEINS

(i) *Chemistry*

Currently, there are only two well characterized representatives in this class of iron–sulfur proteins. They are found in two different genera of photosynthetic bacteria, *Chromatium* and *Rhodopseudomonas*[44,49]. Both have a molecular weight of *ca.* 10,000 and each contain four cysteine residues which presumably are bound to the 4Fe–4S* site. They undergo reversible oxidation and reduction with an unusually high redox potential, *ca.* +330 mV; thus they are referred to as "high-potential iron proteins" (HiPIP).

A peculiarity of these proteins is that the iron is bound to them very tightly. On aminoethylation of the four cysteine residues or treatment of the protein with 8M urea, pH 6.0[44], acid-labile sulfur is released without the simultaneous loss of the iron, which remains tightly bound to the protein. Presently, there are no methods (*a*) to remove the iron from the protein without destroying the protein itself or (*b*) to reconstitute the native protein from the Fe–apoprotein with Na_2S.

Spectrophotometric titrations of the fully reduced *Chromatium* protein with potassium ferricyanide in the presence of oxygen[49] or anaerobic titration of the fully oxidized protein with dithionite[92] show that one electron is transferred during oxidation–reduction.

(ii) *Optical spectroscopy*

The absorption spectrum[44,49] of oxidized *Chromatium* HiPIP shows a very broad band in the visible with shoulders at about 450, 375 and 325 nm. Upon reduction, the visible absorption decreases substantially, and a distinct band with a maximum at 388 nm appears. Both oxidized and reduced forms show strong bands at 283 nm, with relatively little difference in magnitude between the two oxidation states. The 280 nm absorbance is about twice that expected from the aromatic amino acid content[44], indicating a substantial contribution from the iron–sulfur chromophore in this region.

CD studies of *Chromatium* HiPIP have been reported[49]. As in the case of the other iron–sulfur proteins, the CD curves reveal many more spectral features than are apparent from the absorption curve. The CD curves are shown in Fig. 11. It is clear that a number of components underlie the broad visible absorption band characteristic of the oxidized form, and that the reduced form also shows some long-wavelength bands. As Flatmark and Dus point out, the oxidized and reduced forms differ most strongly in the visible region, while in the UV, the two forms show only quantitative differences.
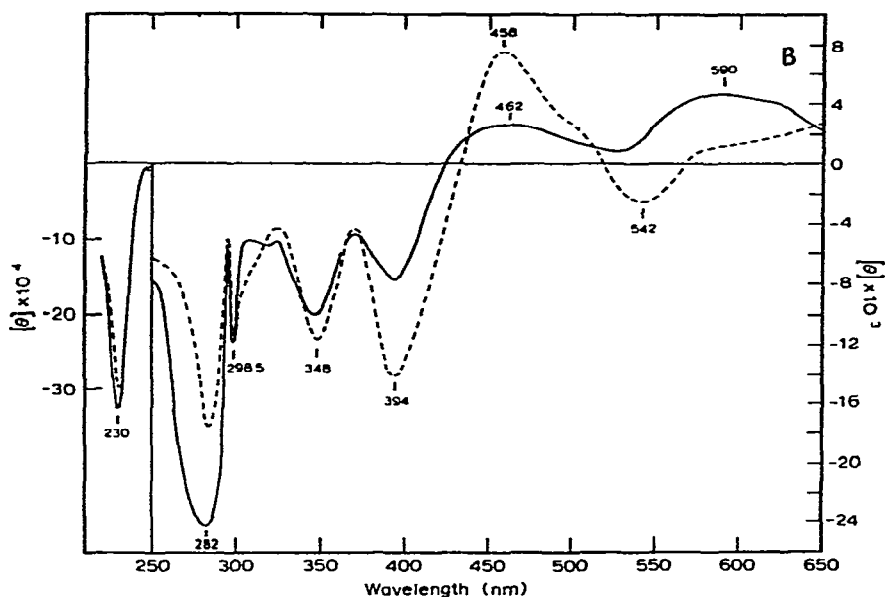
Fig. 11. CD spectra of Chromatium HiPIP oxidized (———) and reduced (— — —)[49] (Courtesy of Elsevier Publishing Co)

(iii) EPR and magnetic susceptibility

HiPIP has unique EPR characteristics among the known iron–sulfur proteins containing more than one iron[115], in that it is the oxidized form which shows EPR signals, while the reduced form shows none. Oxidized HiPIP exhibits an axially-symmetric EPR signal with $g_{\parallel} = 2.12$, $g_{\perp} = 2.04$. The signal is strongly temperature-dependent, being detectable at 28 °K or lower, but not at 76°K. It should be noted that all of the g-values lie above the free-electron value in this case. Quantitative EPR measurements[115] indicate that oxidized HiPIP has one unpaired electron per mole of protein.

Magnetic susceptibility measurements on Chromatium HiPIP have been reported by Ehrenberg and Kamen[45a] and by Moss et al.[101]. These are in good agreement with the EPR data. The oxidized form is paramagnetic, showing Curie-law behavior from 4 °K to 200 °K, with a magnetic moment consistent with $S = 1/2$. The reduced form is diamagnetic within experimental error.

(iv) Mössbauer spectroscopy

Mössbauer spectroscopy has also been applied to Chromatium HiPIP[11,100]. Oxidized HiPIP shows a strongly temperature-dependent spectrum with two sharp quadrupole components observable at 77 °K, which broaden strongly at lower temperatures until at 4.6 °K only a diffuse, unresolved pattern can be seen. This

broadening is attributable to increasing relaxation times for electron-spin-lattice interactions and is consistent with the paramagnetism of the oxidized state. The reduced form shows only minor temperature variation between 77 °K and 4 °K, with well-defined quadrupole split components at both temperatures. Bearden et al.[11] conclude that the quadrupole splitting and isomer shift of the reduced form are compatible with low-spin Fe^{II}.

The most interesting feature of the Mossbauer data for HiPIP is that all four irons appear to be equivalent in both oxidized and reduced forms. Given the fact that only one electron is involved in the reduction and that it is the oxidized form which is paramagnetic, this implies a large degree of delocalization of the "hole" in the oxidized form.

(v) X-ray diffraction

Preliminary X-ray crystallographic studies of reduced *Chromatium* HiPIP have been reported[75,130]. At a resolution of 4 Å, only one very prominent region of high electron density can be seen. In addition, this is the only region which shows appreciable anomalous scattering of CuK_α X-rays to be expected from iron. This implies that the four iron atoms are in a single compact cluster. Strahs and Kraut rule out models in which the irons are well-separated, are in two pairs or are in a linear array. They argue that 1–2–1 or 1–3 arrangements are unlikely and favor a compact structure, possibly tetrahedral in arrangement.

(vi) Discussion

The spectroscopic methods (especially Mossbauer) and X-ray data both seem to point to a structure for HiPIP in which the four irons and four sulfurs are all in close proximity. The apparent equivalence of the four irons in both oxidation states and the iron–sulfur stoichiometry would be neatly accounted for by a tetra-hedral structure of irons with sulfurs above each face. However, the oxidation state of the iron, the number and nature of other ligands present and whether the iron is high-spin or low-spin remains unclear.

E. $nFe–nS^*$ PROTEINS (n MAY RANGE FROM 6–8)

(i) Chemistry

This class consists of bacterial proteins of small molecular weight, *ca.* 6,000, and with high iron and inorganic sulfur content, reported values ranging from 6–8 atoms each per molecule of protein[8,52,82,113]. The protein from *Clostridium pasteurianum* was the protein for which the name "ferredoxin" was coined[98].

Many of the properties of these iron–sulfur proteins are quite similar to those of the 2Fe–2S* type. However, they seem to be somewhat heterogeneous and there are conflicting reports on their molecular weight[82] and Fe, S* content[98].

Amino acid sequences for three bacterial ferredoxins have been determined[19,136,144]. The 8 cysteines appear in identical positions in all three proteins and appear in two clusters of four each, with neighboring cysteines separated by either 2 or 3 amino acids. It is probable that this arrangement has structural significance for the iron–sulfur center.

The number of reducing equivalents transferred during oxidation–reduction is not agreed upon. Values of one[133] and two[92,129] have been reported. There is more evidence for the latter. The redox potential, *ca.* −410 mV at pH 7, was reported[129] to decrease linearly from pH 5.5–9.0. Another group reports it to be independent of pH around neutrality[134].

The reactivity of clostridial ferredoxin with iron chelating and sulfhydryl reagents has been studied extensively[85,86]. This work shows that the iron environment is not readily accessible to chelating agents; however, in the presence of oxygen (which denatures the protein by reacting mainly with the acid-labile sulfur atoms) and/or urea, these agents chelate most or all of the iron atoms present.

It is now agreed[8,85] that the H_2S evolving upon acidification of ferredoxins comes from an "inorganic" form of sulfur and not from cysteine residues by β-elimination.

Clostridial ferredoxin has 8 cysteine residues that are titratable with *p*-chloromercuribenzoate and can be alkylated by iodoacetate[52,82] when urea is present; no free sulfhydryl groups are detectable in the native protein.

(ii) Optical spectroscopy

The absorption spectrum of oxidized bacterial ferredoxins show maxima at 390 and 280 nm and a feature at about 300 nm of variable intensity depending upon the species[43,82,92,96]. In the reduced state, the 390-nm maximum vanishes, and absorption in the visible is generally reduced but not abolished. There is a monotonic rise in absorbance with a maximum at 280 nm. In both oxidation states, a long featureless tail extends all the way into the near IR. Wilson[151] studied the red and near IR spectral region of *Clostridium acidi-urici* ferredoxin at liquid nitrogen temperatures.

Druskeit *et al.*[43] studied the pH-dependence of the absorption spectrum of oxidized *C. pasteurianum* ferredoxin. They observed significant changes in the extinction coefficients on either side of a pH range from about pH 6–9. Further studies of this type need to be carried out to determine whether the observed absorbance changes result from proton dissociation of the intact molecule or from reversible dissociation of iron and/or sulfide.

ORD[55,79] and CD[1,51] spectra have been reported for various bacterial

ferredoxins. Gillard et al.[55] commented on the qualitative similarity of the ORD spectra of bacterial ferredoxin and rubredoxin, and suggested that the chromophores in the two types of proteins may be in rather similar environments. Lovenberg[79] pointed out that the rotations due to bacterial ferredoxins are so much weaker than those of rubredoxin that contamination of ferredoxin by rubredoxin could account for the observed ORD of ferredoxin. However, CD measurements of Atherton et al.[1] show that the similarity in the shape of the ORD curves of rubredoxin and ferredoxin was largely fortuitous and that there are both quantitative and qualitative differences in the CD spectrum. They maintain that in certain wavelength regions, the CD curves are suggestive of similarities between the two types of chromophore.

As in the case of the 2Fe–2S* systems, both oxidized and reduced forms of *Peptostreptococcus elsdenii* ferredoxin show CD at wavelengths in the visible where there are no obvious absorption features, thereby revealing additional detail in the electronic spectra. Atherton et al.[1] speculate that the lower magnitude of the CD bands in bacterial ferredoxins relative to those of rubredoxin may result from a lower helix content of ferredoxin. As we have noted in our discussion of rubredoxin, the evidence for any substantial helix content in this case is weak. Furthermore, there is no reason to expect any strong correlation between helix content and the magnitude of extrinsic Cotton effects.

(iii) EPR and magnetic susceptibility

EPR signals for a bacterial ferredoxin were first detected by Palmer et al.[113] in reduced *C. pasteurianum* ferredoxin at 15 °K. They reported apparent g-values of 1.892, 1.960 and 2.005, i.e., the spectrum is of the rhombic type. They pointed out that this EPR signal is more complex than those of other iron–sulfur proteins and called attention to the presence of shoulders at each end of the spectrum. The complexity could be attributable to heterogeneity, either intra- or intermolecular, or possibly to dipole–dipole coupling between neighboring paramagnetic centers. The signal intensity of bacterial ferredoxins, like those of plant ferredoxins, is very temperature sensitive, and cannot be detected at liquid nitrogen temperatures.

Recently, Orme-Johnson and Beinert[106] have described EPR experiments which indicate that as increasing amounts of dithionite are added to *C. pasteurianum* ferredoxin, two distinct types of EPR signals can be detected. Initially a pattern with $g_{\parallel} = 2.06$, $g_{\perp} = 1.94$ is observed but as this pattern continues to grow, a narrower signal appears near $g = 2$. Both signals are completely developed when two reducing equivalents have been added per mole of protein, and the relative areas under the two signals are comparable. This is consistent with two types of centers, each accepting one electron. Orme-Johnson and Beinert[106] point out that in the 2Fe–2S* systems, one electron is taken up by two iron atoms, and that if this holds also for the case of bacterial ferredoxins with 8 irons, there must

be an additional type of iron which does not contribute to the EPR signal. However, one could also envision two 4-center clusters, each taking up one electron, similar to the situation in HiPIP.

Magnetic susceptibility studies of *C. pasteurianum* ferredoxin were first reported by Blomstrom *et al.*[21], and more recently by Druskeit *et al.*[43]. Blomstrom *et al.* found an average magnetic moment per iron of 2.0–2.3 Bohr magnetons in the oxidized state (assuming 7 Fe/mole), which is consistent with low-spin Fe^{III}. Within experimental error and allowing for reasonable variation in the magnetic moment of low-spin Fe^{III}, up to three low-spin Fe^{II} could be present per mole, but Blomstrom *et al.* argued that Mössbauer and chelation studies point to all seven irons being low-spin Fe^{III}. Druskeit *et al.*[43] studied the pH dependence of the magnetic susceptibility. They observed between pH 6 and 8 a minimum in the susceptibility per iron.

Recently, Poe *et al.*[118] have studied the temperature dependence of the magnetic susceptibility of clostridial ferredoxin in solution using a 220-MHz NMR spectrometer. In the oxidized state, the susceptibility per iron shows a linear *increase* with temperature over the range from 6–65 °C, indicating strong anti-ferromagnetic coupling between irons. As the number of irons per molecule is not known with certainty, the effective moment per iron could not be determined precisely. However, for either 6 or 8 irons, the moment per iron is less than the value of 1.73 Bohr magnetons expected for low spin Fe^{3+}. A limiting value of μ_{eff} of 1.73 B.M. is not inconsistent with the data, although a limiting value corresponding to high spin Fe^{3+} cannot be ruled out.

The reduced form exhibits the expected Curie-law behavior. The increase in susceptibility on reduction corresponds to an effective moment of 3.0 B.M. per electron added, assuming a two-electron reduction.

(iv) Mossbauer spectroscopy

Mössbauer spectroscopic studies of oxidized clostridial ferredoxin were performed by Blomstrom *et al.*[21] (see also Phillips *et al.*[116]). Quadrupole splittings varied with temperature from 0.93 mm/sec at 77 °K to 0.70 mm/sec at 298 °K. The slightly asymmetric signals suggested two overlapping components with similar isomer shifts and quadrupole splittings, whose proximity prevented an exact determination of the relative numbers of irons contributing to the two signals. They found that two components with a ratio of 5:2 could account for their data, and suggested a model which consisted of a linear array of seven irons bridged by S* and cysteine R–S ligands. Blomstrom *et al.* proposed that all seven irons were low-spin Fe^{III}, consistent with their magnetic susceptibility data and Mössbauer parameters. The two types of iron seen in Mössbauer were assigned to terminal (2 irons) and internal (5 irons) atoms in the linear array.

Mössbauer studies of another bacterial ferredoxin from *Chromatium* have

also been reported[11,100]. In the oxidized form, the spectrum reported was similar to that found by Blomstrom *et al.* for *Clostridium* ferredoxins, with two super-imposed signals with the same isomer shift but different quadrupole splittings. They assign these to two different types of Fe^{III} and estimate a 1:2 ratio, with the more widely split pair being the more intense. On reduction with dithionite, about 1/6 of the total iron appears as a widely split quadrupole pair (2 87 mm/sec quadrupole splitting at 77 °K) and having an isomer shift of +1.15 mm/sec relative to ^{57}Co in copper. The large values for the isomer shift and quadrupole splitting lead them to assign this signal to high-spin Fe^{II}.

(v) NMR

Poe *et al.*[118] have made NMR studies of clostridial ferredoxin at 220 MHz. They find resolvable proton signals at low fields showing temperature dependence characteristic of contact-shifted protons in both the oxidized and reduced forms. In the oxidized form, a total of 16 contact-shifted protons can be distinguished, with one set of 8 protons having roughly twice the spin density of another set of 8. Poe *et al.* assign these to the β-CH_2 protons of cysteine and suggest that the 4 cysteines whose protons are shifted to lowest fields are bonded to two iron atoms each, and the other four cysteines are bonded to one iron atom each. Poe *et al.* propose a model consistent with these observations (Fig. 12).
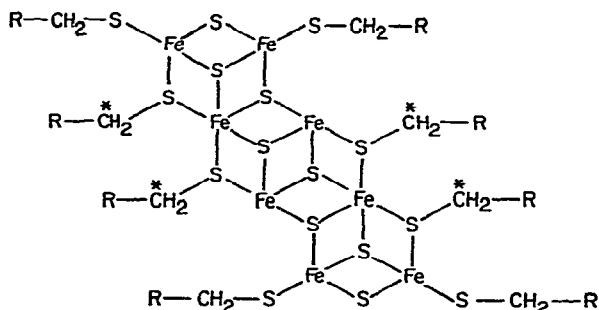

Fig. 12   Model for iron–sulfur complex in *C pasteurianum* ferredoxin proposed by Poe *et al.*[118]. (Courtesy of National Academy of Sciences, U.S A.)

In the reduced form, contact-shifted protons can also be observed, although the signals are much broader and were not analyzed in detail.

In partially reduced ferredoxin the broadening of proton resonance lines suggests rapid intermolecular electron exchange between oxidized and reduced forms (rate constants of the order of 10^7 $sec^{-1} \cdot M^{-1}$).

(vi) *X-ray diffraction*

Sieker and Jensen[127] have reported a preliminary study of the ferredoxin from *Micrococcus aerogenes*. The Patterson map obtained at 5 Å resolution was not consistent with the linear array of seven irons proposed by Blomstrom *et al.*[21], but does not rule out shorter linear arrays or a non-linear cluster containing all of the irons.

(vii) *Discussion*

The evidence from EPR and Mossbauer spectroscopy points to the presence of at least two types of iron in bacterial ferredoxins. This could either be interpreted, following Blomstrom *et al.*[21] as terminal and central members of a single array or as two or more smaller clusters. The X-ray data argue against a single linear array but a non-linear array could be present, as in the model proposed by Poe *et al.*[118]. The observation of two distinct types of EPR signals[106] would seem to be most consistent with two smaller clusters, but is probably not inconsistent with a single cluster.

F. IRON–SULFUR FLAVOPROTEINS

(i) *Chemistry*

The iron–sulfur flavoproteins present even more complex structural problems than the iron-sulfur proteins we have previously discussed. In addition to a large number of iron and labile sulfur atoms (≥ 4 of each) and one or more flavins, some contain molybdenum. The best characterized proteins in this class are xanthine oxidase, dihydroorotic dehydrogenase, aldehyde oxidase, succinic dehydrogenase and DPNH dehydrogenase. We shall concentrate here on those properties which are related to the structure of the iron–sulfur center in these enzymes, particularly xanthine oxidase, which has been studied more thoroughly than the others.

(ii) *Optical spectroscopy*

The absorption spectrum of xanthine oxidase was first reported by Corran *et al.*[33] to be significantly different from that of a typical flavin. Rajagopalan and Handler[119] showed that xanthine oxidase, aldehyde oxidase and dihydroorotic dehydrogenase, while having non-identical absolute spectra, gave very similar difference spectra when the contribution of the flavin moiety was subtracted and the spectrum placed on a per iron basis. Very recently, Komai *et al.*[74] have re-

ported a new method for removing flavin from xanthine oxidase. Qualitatively, the spectra of this deflavoxanthine oxidase are very similar to those of the 2Fe–2S* proteins. On the basis of extinction coefficient per iron atom, the spectra are also quantitatively similar, except at the longest wavelength maximum in the oxidized form where xanthine oxidase has a 20–30% higher extinction coefficient. As Komai et al. point out, this may reflect either some difference in the iron–sulfur environment, or contributions from the molybdenum center which is present. In any event, the results of Komai et al. suggest that there are no major perturbations of the flavin spectra on binding to the enzyme, that the molybdenum center does not make a major contribution to the absorption spectrum and that the iron–sulfur chromophore(s) is (are) similar to those in 2Fe–2S* proteins.

Massey et al.[90] have examined the kinetics of spectral changes upon anaerobic reduction of xanthine oxidase by xanthine, various substrate analogues and dithionite. All of these reductions show biphasic kinetics. In the initial fast step, 4 electrons are taken up per flavin and the results of Massey et al. combined with EPR studies by Bray et al.[25], to be described below, suggest that 2 electrons reduce FAD to $FADH_2$, one reduces Mo^{VI} to Mo^V and that the fourth is taken up by the Fe–S* center(s). Three or four electrons are involved in the slow step, depending on whether substrate or dithionite is used as a reductant. Of these one presumable goes into the Fe–S* center(s), but two possible distributions for the remaining 2 or 3 are suggested by Massey et al Studies of deflavo xanthine oxidase by Komai et al.[74] are consistent with the above results.

Circular dichroism spectra for xanthine oxidase have been reported by Garbett et al[51] and by Palmer and Massey[110]. Qualitatively the CD spectra of xanthine oxidase in the visible range resemble closely those of spinach ferredoxin. As pointed out by Palmer and Massey, a consideration of individual bands obtained upon analysis into Gaussian components indicates an even stronger similarity than does an examination of the unresolved curves. These results suggest that the Mo centers and the flavins do not contribute significantly to the CD They also imply that the iron–sulfur chromophores in xanthine oxidase are structurally similar to those of spinach ferredoxin.

The minor role of flavin in the xanthine oxidase CD is further borne out by measurements[74] of the CD spectra of deflavoxanthine oxidase (oxidized and reduced) which show strong similarities to those of the native enzyme. This is especially striking in the oxidized form, where the two forms are virtually identical. The reduced forms show more variation, but it is probable that a consideration of the individual bands would show only quantitative differences, rather than qualitative ones.

Palmer and Massey[110] also observed that the CD spectra of xanthine oxidase reflect the biphasic behavior discussed above in connection with absorption spectra. The circular dichroism at the 433 nm maximum decreased in both the fast and the slow phases by amounts similar to the CD changes on one-electron reduc-

tion of 2Fe–2S* systems[114]. Thus CD also points to heterogeneity of the irons in xanthine oxidase.

The ORD spectrum of a DPNH dehydrogenase has been reported[73]. This enzyme has an ORD spectrum which differs strongly from that of xanthine oxidase[51]. Rotational strengths were calculated from the observed ORD curve, assuming Gaussian CD bands. King et al.[73] conclude that the oxidized and reduced forms show two bands, one at about 436 nm, the other at about 350 nm. These do not shift much on reduction and, surprisingly, the reduced protein shows larger rotational strengths than the oxidized protein. They attribute these bands to the flavin moiety. It is likely, however, that when this protein is examined by CD, with its greater resolving power, more bands will be detected and the Fe–S* chromophore will probably also be found to contribute.

(iii) EPR and magnetic susceptibility

Xanthine oxidase has been extensively studied by EPR. Bray[23], Beinert and Palmer[14], and Bray et al.[26] have summarized the earlier work on this enzyme. The presence of three EPR active centers in this enzyme makes EPR spectroscopy both interesting and complicated Using a rapid freezing technique to follow fast kinetics, Bray et al.[25] presented convincing evidence that the order of reduction is Mo → flavin → iron. The iron signals observed in this system[53,106,110,112] show g-values very similar to those observed in 2Fe–2S* systems ($g_z = 2.022$, $g_x = 1.899$, $g_y = 1.935$ according to Gibson and Bray[53]) The more recent studies[53,106,110] indicate that at very low temperatures ($< 30\ °K$) another EPR signal is present at $g = 2.11$ in xanthine oxidase. This is also presumably due to the Fe–S* system. The exact number of electrons involved in the production of this new type of EPR signal *vs.* the "classical" $g = 1.94$ signal, and the time sequence of their appearance requires further investigation. At the least, these results point to heterogeneity of the irons in xanthine oxidase. Apparently, two types of iron–sulfur groups are present with distinct EPR characteristics but with similar optical properties.

Rajagopalan et al.[120,121] have reported very thorough EPR studies of aldehyde oxidase, which shows many similarities to xanthine oxidase. The Fe–S* center(s) give EPR signals resembling those of xanthine oxidase and 2Fe–2S* proteins. Rapid freezing experiments point to the same sequence of reduction: Mo → flavin → Fe–S* Here also only one electron appears to be required for four irons in order to develop the maximal $g = 1.94$ signal, but further optical changes occur on addition of reductant beyond that point. It is likely that further investigation at very low temperatures will reveal a $g = 2.1$ signal analogous to that recently detected in xanthine oxidase[106,110].

Magnetic susceptibility measurements on xanthine oxidase have been reported[24,45]. The oxidized enzyme has a net diamagnetism but depending on how

one corrects for the protein contribution, one can obtain a small degree of para-magnetism. Ehrenberg and Bray argue that the weak paramagnetism indicates that most of the irons are low-spin Fe^{II}, but that some (perhaps 2 out of 8/mole protein) are low-spin Fe^{III}. On complete reduction with dithionite, the susceptibility becomes more positive by an amount consistent with about 2 irons going from Fe^{III} (low spin) to Fe^{II} (high spin). Such a change would almost certainly require substantial alterations in the ligation about the iron (number, nature and/or distance of ligands) for spin pairing is much more difficult in d^5 (ferric) complexes than in d^6 (ferrous) complexes[48]. Coupling within pairs or larger groupings of iron could make the susceptibility data consistent with all 8 irons being Fe^{III} (either high or low spin) in the oxidized state.

(iv) Mössbauer spectroscopy

Mössbauer spectra of xanthine oxidase have been reported[66,68]. These spectra indicate that all the irons in xanthine oxidase are equivalent in both the oxidized and the reduced state. Furthermore, the spectra are very similar to those for spinach and Euglena ferredoxins.

(v) Discussion

The optical, spin resonance and Mössbauer data all suggest that the Fe–S* centers present in xanthine oxidase closely resemble those in 2Fe–2S* proteins. The most plausible model is that the 8Fe–8S* are present as 2Fe–2S* centers with structures similar to those in green plant ferredoxins. EPR data have recently pointed to the conclusion that the 2Fe–2S* centers are not exactly identical, but the difference must be sufficiently subtle as to escape ready differentiation by optical and Mössbauer techniques. For other iron–sulfur flavoproteins, the data are much less complete, but it is not improbable that similar pairing occurs. As the structure of the 2Fe–2S* systems becomes better understood, more rapid progress should be possible with these complex proteins.

G. NITROGENASES

The reduction of N_2 by multienzyme systems, the nitrogenases, has received a great deal of attention[58,103]. It has been shown that nitrogenases consist of two proteins, one containing molybdenum, iron and acid-labile sulfur and the other iron and acid-labile sulfur. The Fe–S* component, which Mortenson *et al.*[99] refer to as azoferredoxin, has some spectral and chemical properties[59,102] similar to those of Fe–S* proteins from other systems (*cf.* previous sections). However, the two iron atoms in azoferredoxin are not equivalent and there is no EPR signal

unless the protein is oxidized[97]. Novikov *et al.*[105] reported an EPR signal ($g_\perp$ = 1.93 and $g_\parallel$ = 2.01) of the nitrogenase from *Azotobacter vinelandii* after reduction with dithionite. They also report the Mössbauer spectrum of the same protein.

Now that the nitrogenase components can be obtained in pure form it will be possible to see how many similarities exist between the Fe–S* components of the N_2 and O_2 reducing systems.

H. MODEL SYSTEMS

A major difficulty in interpreting the physical properties of the iron-sulfur proteins has been the lack of simple coordination complexes which can serve as adequate models. An ideal model system would be one in which iron is coordinated by sulfur-containing ligands in which the sulfur is not part of an extended π-electron system and in which well-defined binuclear and/or polynuclear complexes can be formed. Several types of model systems have been examined but none have all of the above-mentioned properties.

Numerous mononuclear complexes of iron with sulfur-containing ligands have been synthesized and studied[70,78]. The complexes which have been examined most thoroughly by spectroscopic techniques are the dithiocarbamates and dithiophosphates[35], and the dithiolene derivatives[94]. Unfortunately in these ligands the sulfurs participate in a conjugated chelate ring system, although Jørgensen[69] argues that the extent of conjugation in the dithiocarbamates and dithiophosphates is small.

Turning to models for dimeric systems, several interesting types have been examined. Dithiolene complexes of Fe and other transition metals form dimers in which the metal of one planar bisbidentate unit is coordinated by the sulfur in the other planar unit[6,39], as shown in Fig. 13.

Dahl and co-workers[38,147] have determined the structures of a number of interesting iron carbonyl–sulfur complexes, *e.g.*, $[Fe(CO)_3S]_2$ and
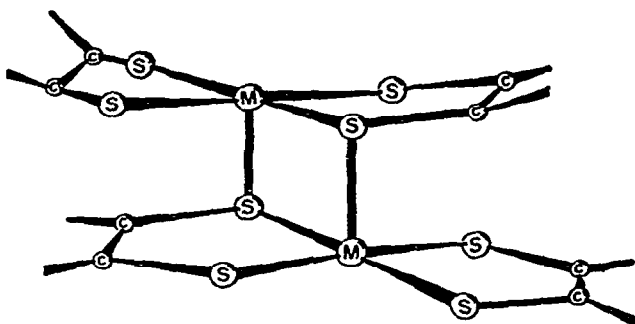

Fig. 13   Structure of a dimeric dithiolene complex[39]. (Courtesy of American Chemical Society.)

$[Fe(CO)_3SC_2H_5]_2$. This type of molecule (which may be envisioned as having a bent iron–iron bond) and the related Roussin's red esters[137] $[(NO)_2FeSR]_2$ have been mentioned as possible models for iron–sulfur centers in proteins[8,21]. This model certainly deserves further consideration, although it is difficult to see how typical protein ligands can substitute for CO and NO as the efficient electron acceptors required to stabilize the low oxidation levels characteristic of these carbonyl and nitrosyl derivatives.

Probably the most interesting model compounds for dimeric iron–sulfur systems described to date is the complex $[Fe(S_2CSC_2H_5)_2(SC_2H_5)_2]_2$. The preparation and crystal structure determination of this complex was reported by Coucouvanis et al.[36] The structure of this molecule is shown in Fig 14. The complex contains Fe^{III} (at least in the formal sense), but is diamagnetic. The thioxanthate ligands are certainly non-physiological, but one could at least envision their replacement by typical protein groups Optical and EPR studies of this molecule and/or its reduction products should be of great interest.
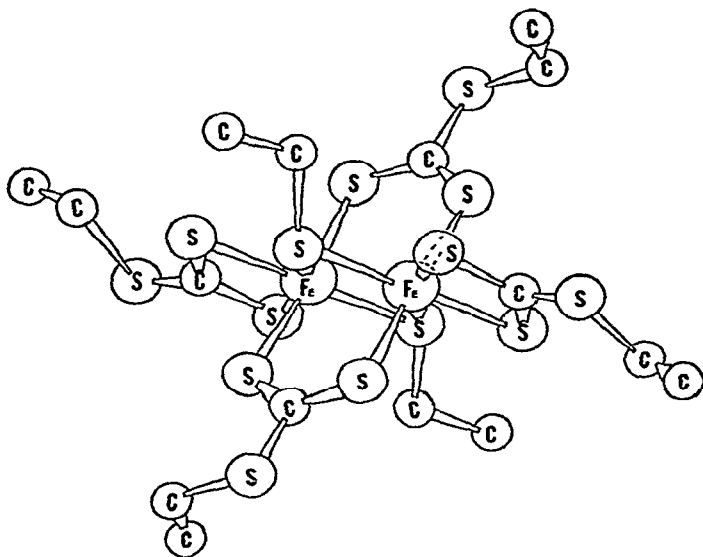

Fig 14   Structure[36] of the complex $[Fe(S_2CSC_2H_5)_2(SC_2H_5)]_2$ (Courtesy of American Chemical Society.)

Models for tetranuclear iron–sulfur complexes are rare and appear to be confined at present to cyclopentadienyl[124,148] and nitrosyl (Roussin's black salt)[64] derivatives.

As a limiting form of polynuclear iron–sulfur complexes, we have a number of crystalline substances such as iron pyrite and marcasite (FeS_2), $KFeS_2$, etc.

A completely different type of model compound has been recently explored

by Suzuki and Kimura[132] and McCarthy and Lovenberg[93]. Suzuki and Kimura showed that on incubation with Fe^{II} and mercaptoethanol, bovine serum albumin (BSA) forms a complex with a visible and near ultraviolet absorption spectrum with a maximum at 386 nm and broad peaks at 327 and 630 nm, and having extinction coefficients per iron comparable to those of ferredoxins.

These observations were extended by McCarthy and Lovenberg[93] who found that complexes with BSA could be formed by adding only a ferrous salt, or by adding a ferrous salt together with either mercaptoethanol or a ferrous salt plus mercaptoethanol plus sodium sulfide. These three complexes showed distinctive absorption and CD spectra. Of the three types of complex, the one formed with Fe^{II}, mercaptoethanol, and sulfide resembled the ferredoxins most closely in absorption spectra, showing maxima at 320 and 415 nm and shoulders at 460 and 520 nm. The CD spectrum of this complex is much weaker than that of rubredoxin or adrenodoxin, and has amplitudes comparable to those of bacterial ferredoxins, although the signs and positions of the extrema are quite dissimilar to all three natural iron–sulfur proteins.

Yang and Huennekens[154] have recently reported the preparation of iron–sulfur complexes with soybean trypsin inhibitor and ribonuclease which resemble those formed with BSA. They also describe a reaction of Fe^{III}, mercaptoethanol and S^{2-} to form an unstable complex which shows absorption maxima at 318 and 412 nm and shoulders at about 460 and 520 nm. The Fe: inorganic sulfide stoichiometry was deduced to be 1:1. In the absence of oxygen, the complex could only be formed with Fe^{III}, but if oxygen was present, Fe^{II} sufficed. It was also observed that the absorbance at 318 and 412 nm decreased slowly with time, but could be regenerated by aeration. These observations suggest that the visible absorption bands should be attributed to iron in the Fe^{III} state. EPR signals at $g = 4.1$ were observed presumably due to high-spin Fe^{III}, with weak signals near $g = 2$ attributed to a transient species. Unfortunately, attempts to isolate this complex failed.

authors cited in the legends. We are grateful to these authors and to the publishers of the various journals for their permission to reproduce these figures here.

REFERENCES

1 N M ATHERTON, K. GARBETT, R. D GILLARD, R MASON, S J MAYHEW, J. L PEEL AND J E. STANGROOM, *Nature*, 212 (1966) 590
2 H BACHMAYER, L H PIETTE, K. T. YASUNOBU AND H R WHITELEY *Proc Nat Acad Sci. U.S.*, 57 (1967) 122.
3 H BACHMAYER, A M. BENSON, K. T YASUNOBU, W. T. GARRAD AND H. R WHITELEY, *Biochem*, 7 (1968) 986
4 H BACHMAYER, K. T. YASUNOBU, J L PEEL AND S MAYHEW, *J Biol Chem*, 243 (1968) 1022.
5 H. BACHMAYER, K. T. YASUNOBU AND H R WHITELEY, *Proc. Nat. Acad. Sci U S*, 59 (1968) 1273
6 A L BALCH, I G. DANCE AND R H HOLM, *J Amer Chem Soc*, 90 (1968) 1139
7 E BAYER, R PARR AND B KAZMAIER, *Arch Pharm*, 298 (1965) 196.
8 E BAYER, H. ECKSTEIN, H HAGENMAIER, D JOSEF, J KOCH, P KRAUSS, A ...'ODER AND P SCHRETZMANN, *Eur. J. Biochem*, 8 (1969) 33
9 E BAYER, H A O HILL, A RODER AND R. J P WILLIAMS, *J. Chem Soc. (D)* (1969) 109
10 A J. BEARDEN AND T H MOSS, in A EHRENBERG, B G MALMSTROM AND T. VÁNNGARD (Eds), *Magnetic Resonance in Biological Systems*, Pergamon Press, Oxford, 1967, p 391.
11 A J. BEARDEN, T. H. MOSS, R G. BARTSCH AND M A CUSANOVICH, in A. SAN PIETRO (Ed), *Non-Heme Iron Proteins*, Antioch Press, Yellow Springs, Ohio, 1965, p 87.
12 H BEINERT in E C SLATER (Ed), *Flavins and Flavoproteins*, Elsevier, Amsterdam, 1966, p 49
13 H BEINERT AND W. H. ORME-JOHNSON, *Ann N Y Acad Sci*, 158 (1969) 336
14 H. BEINERT AND G PALMER, *Advan Enzymol Relat. Subj Biochem*, 27 (1965) 105
15 H BEINERT AND R H SANDS, *Biochem Biophys Res Commun*, 3 (1960) 41.
16 H BEINERT, W. HEINEN AND G PALMER, *Brookhaven Symposia in Biology, U S. Atom. Energy Comm*, 15 (1962) 229
17 H BEINERT, P. HEMMERICH, D. V DERVARTANIAN, C VEEGER AND J D. W. VAN VOORST, *Biochim. Biophys. Acta*, 96 (1965) 530
18 A M BENSON AND K. T YASUNOBU, *J Biol Chem*, 244 (1969) 955
19 A. M. BENSON, H. F. MOWER AND K T YASUNOBU, *Proc. Nat Acad Sci U S*, 55 (1966) 1532.
20 B. BLEANEY AND K D. BOWERS, *Proc Roy. Soc (London)*, A214 (1952) 451.
21 D C. BLOMSTROM, E. KNIGHT, JR., W. D. PHILLIPS AND J. F. WEIHER, *Proc Nat. Acad Sci U S*, 51 (1964) 1085
22 W. E BLUMBERG AND J PEISACH, in A SAN PIETRO (Ed), *Non-Heme Iron Proteins*, Antioch Press, Yellow Springs, Ohio, 1965, p. 101.
23 R. C. BRAY, in P. D BOYER, H LARDY AND K. MYRBACK (Eds), *The Enzymes*, Vol. 7A, Academic Press, New York, 1963, p 533
24 R. C. BRAY, R PETTERSSON AND A EHRENBERG, *Biochem J*, 81 (1961) 178
25 R. C. BRAY, G. PALMER AND H BEINERT, *J Biol Chem*, 239 (1964) 2667
26 R C BRAY, G. PALMER AND H BEINERT, in T E KING, H S MASON AND M MORRISON (Eds), *Oxidases and Related Redox Systems*, vol I, Wiley, New York, 1965, p 359
27 H BRINTZINGER, G. PALMER AND R H SANDS, *J Amer. Chem Soc*, 88 (1966) 623
28 H. BRINTZINGER, G. PALMER AND R H SANDS, *Proc Nat Acad Sci U S*, 55 (1966) 397.

29 B. B BUCHANAN, *Struct. Bonding (Berlin)*, 1 (1966) 109.

30 T. CASTNER, JR , G S NEWELL, W. C HOLTON AND C P. SLICHTER, *J Chem Phys*, 32 (1960) 668

31 R. COOKE, J. C M TSIBRIS, P G. DEBRUNNER, R L TSAI, I C. GUNSALUS AND H FRAUEN-FELDER, *Proc. Nat. Acad. Sci. U.S*, 59 (1968) 1045.

32 M J. COON, 1969, private communication

33 H. S CORRAN, J. G. DEWAN, A. H. GORDON AND D E. GREEN, *Biochem. J.*, 33 (1939) 1694.

34 F. A. COTTON AND G. WILKINSON, *Advanced Inorganic Chemistry*, 2nd ed., Wiley, N Y., 1966, p 671

35 D. COUCOUVANIS, *Progr. Inorg. Chem*, 11 (1970) 233.

36 D. COUCOUVANIS, S J. LIPPARD AND J A ZUBIETA, *J Amer. Chem. Soc*, 91 (1969) 761.

37 D W. CUSHMAN, R. L TSAI AND I C GUNSALUS, *Biochem Biophys Res Commun*, 26 (1967) 577.

38 L. F. DAHL AND C. H WEI, *Inorg. Chem*, 2 (1963) 328

39 A DAVISON, D W HOWE AND E T. SHAWL, *Inorg Chem*, 6 (1967) 458

40 P. G. DEBRUNNER, in D. W. URRY (Ed.), *Spectroscopic Approaches to Biomolecular Conformation*, American Medical Association, 1970, p 209

41 D. V. DERVARTANIAN, W. H ORME-JOHNSON, R E HANSEN, H BEINERT, R L TSAI, J C M TSIBRIS, R C BARTHOLOMAUS AND I C GUNSALUS, *Biochem Biophys Res. Commun*, 26 (1967) 569.

42 R. E DICKERSON, M. L. KOPKA, J WEINZIERL, J VARNUM, D. EISENBERG AND E MARGOLIASH, *J. Biol Chem*, 242 (1967) 3015

43 W. DRUSKEIT, K GERSONDE AND H NETTER, *Eur J Biochem*, 2 (1967) 176

44 K. DUS, H. DE KLERK, K SLETTEN AND R G BARTSCH, *Biochim. Biophys Acta*, 140 (1967) 291.

45 A EHRENBERG AND R. C BRAY, *Arch Biochem Biophys*, 109 (1965) 199.

45a A EHRENBERG AND M D. KAMEN, *Biochim Biophys Acta*, 102 (1965) 333.

46 R W. ESTABROOK, International Meeting on Magnetic Resonance, Airlie House, Warrenton, Virginia, 1968

47 R E. FEENEY AND S K. KOMATSU, *Struct Bonding (Berlin)* 1 (1966) 149.

48 B N. FIGGIS, *Introduction of Ligand Fields*, Interscience, New York, N.Y., 1966.

49 T FLATMARK AND K DUS, *Biochim Biophys Acta*, 80 (1969) 377.

50 J. K FOGO AND M POPOWSKY, *Anal Chem*, 21 (1949) 732.

51 K. GARBETT, R D GILLARD, P F. KNOWLES AND J. E STANGROOM, *Nature*, 215 (1967) 824

52 K. GERSONDE AND W. DRUSKEIT, *Eur J Biochem*, 4 (1968) 391

53 J. F. GIBSON AND R. C. BRAY, *Biochim. Biophys. Acta*, 153 (1968) 721.

54 J F GIBSON, D O. HALL, J H M THORNLEY AND F R WHATLEY, *Proc. Nat. Acad. Sci U S*, 56 (1966) 987.

55 R. D. GILLARD, E. D. McKENZIE, R MASON, S G. MAYHEW, J L PEEL AND J. E. STANGROOM, *Nature*, 208 (1965) 769.

56 H A. HARBURY, in B. CHANCE, R W. ESTABROOK AND T. YONETANI (Eds), *Hemes and Hemoproteins*, Academic Press, New York, N Y, 1966, p 391.

57 H A. HARBURY, J R. CRONIN, M W. FANGER, T. P. HETTINGER, A J MURPHY, Y P. MYER AND S N. VINOGRADOV, *Proc. Nat Acad Sci. U S*, 54 (1965) 1658

58 R W. F. HARDY AND R C BURNS, *Ann Rev. Biochem*, 37 (1968) 331

59 R. W. F. HARDY, R C BURNS, K. T FRY AND R D. HOLSTEN, *XI Intern. Bot. Congr*, Abstracts, Seattle, 1969, p. 85.

60 O. HAYAISHI AND M NOZAKI, *Science* 164 (1969) 389.

61 J. R HERRIOTT, L. C. SIEKER, L. H JENSEN AND W LOVENBERG, *J Mol Biol*, 50 (1970) 391.

62 T. C. HOLLOCHER, F. SOLOMON AND T E RAGLAND, *J. Biol Chem*, 241 (1966) 3452

63 J. HONG AND J. C RABINOWITZ, *Biochem Biophys Res Commun*, 29 (1967) 246

64 G. JOHANNSON AND W. N LIPSCOMB, *Acta Cryst*, 11 (1958) 594.

65 C. E JOHNSON AND D. O. HALL, *Nature*, 217 (1968) 446.

66 C E. JOHNSON, P. F KNOWLES AND R C BRAY, *Biochem J*, 103 (1967) 10c.

67 C. E. JOHNSON, E. ELSTNER, J. F. GIBSON, G. BENFIELD, M C. W. EVANS AND D. O HALL, *Nature*, 220 (1968) 1291.

68   C E JOHNSON, R. C BRAY, R. CAMMACK AND D. O. HALL, *Proc. Nat. Acad Sci. U S*, 63 (1969) 1234

69   C K JØRGENSEN, *Inorganic Complexes*, Academic Press, N.Y, 1963, p. 138.

70   C K JØRGENSEN, *Inorg. Chim Acta Reviews*, 2 (1968) 65.

71   S. KERESZTES-NAGY, F. PERINI AND E MARGOLIASH, *J. Biol Chem*, 244 (1969) 981.

72   T. KIMURA, *Struct. Bonding (Berlin)*, 5 (1968) 1.

73   T. E KING, P. M. BAYLEY AND B MACKLER, *J. Biol Chem*, 244 (1969) 1890

74   H KOMAI, V. MASSEY AND G. PALMER, *J. Biol. Chem*, 244 (1969) 1692

75   J KRAUT, G. STRAHS AND S. T. FREER, in A RICH AND N. DAVIDSON (Eds), *Structural Chemistry and Molecular Biology*, Freeman, San Francisco, 1968, p 55.

76   W. KUHN, *Ann Rev. Phys. Chem*, 9 (1958) 417.

77   A. B. P. LEVER, *Inorganic Electronic Spectroscopy*, Elsevier, Amsterdam, 1969, p 241.

78   S E LIVINGSTONE, *Quart Rev (London)*, 19 (1965) 386

79   W. LOVENBERG, *Proc. 14th Coll Protides Biol Fluids*, Bruges, 1966, p. 165.

80   W. LOVENBERG AND B E. SOBEL, *Proc. Nat Acad Sci. U.S.*, 54 (1965) 193.

81   W. LOVENBERG AND W. M. WILLIAMS, *Biochem*, 8 (1969) 141.

82   W LOVENBERG, B. B. BUCHANAN AND J. C. RABINOWITZ, *J. Biol. Chem.*, 238 (1963) 3899.

83   R MALKIN AND J. C. RABINOWITZ, *Biochem*, 5 (1966) 1262.

84   R. MALKIN AND J. C. RABINOWITZ, *Biochem Biophys Res. Commun.*, 23 (1966) 822

85   R MALKIN AND J C RABINOWITZ, *Ann. Rev. Biochem*, 36 (1967) 113.

86   R. MALKIN AND J. C. RABINOWITZ, *Biochem*, 6 (1967) 3880

87   B. G. MALMSTROM AND J. B NEILANDS, *Ann. Rev. Biochem*, 33 (1964) 331.

88   S. F. MASON, *Quart Rev. (London)*, 17 (1963) 20.

89   V. MASSEY, *J. Biol Chem*, 229 (1957) 763.

90   V. MASSEY, P. E. BRUMBY, H. KOMAI AND G. PALMER, *J Biol. Chem.*, 244 (1969) 1682.

91   H MATSUBARA, R. M. SASAKI AND R. K. CHAIN, *J. Biol. Chem.*, 243 (1968) 1725.

92   S. G. MAYHEW, D PETERING, G. PALMER AND G P FOUST, *J Biol. Chem*, 244 (1969) 2830.

93   K. MCCARTHY AND W. LOVENBERG, *J. Biol Chem.*, 243 (1968) 6436

94   J. A MCCLEVERTY, *Progr Inorg. Chem*, 10 (1968) 49.

95   A. S. MILDVAN, R. W. ESTABROOK AND G. PALMER, in A EHRENBERG, B G. MALMSTROM AND T. VANNGARD (Eds.), *Magnetic Resonance in Biological Systems*, Pergamon Press, London, 1967, p 175.

96   L. E MORTENSON, *Biochim. Biophys. Acta*, 81 (1964) 71.

97   L E. MORTENSON, *XI Intern Bot Congr*, Abstracts, Seattle, 1969, p 152.

98   L E. MORTENSON, R C. VALENTINE AND J E CARNAHAN, *Biochem. Biophys. Res. Commun*, 7 (1962) 448.

99   L. E. MORTENSON, J. A. MORRIS AND D. Y. JENG, *Biochim. Biophys. Acta*, 141 (1967) 516.

100   T. H. MOSS, A J. BEARDEN, R. G. BARTSCH, M. A CUSANOVICH AND A. SAN PIETRO, *Biochem*, 7 (1968) 1591.

101   T. H. MOSS, D. PETERING AND G PALMER, *J. Biol Chem*, 244 (1969) 2275.

102   E MOUSTAFA AND L E MORTENSON, *Biochim Biophys. Acta*, 172 (1969) 106

103   R. MURRAY AND D. C. SMITH, *Coordin. Chem. Rev*, 3 (1968) 429.

104   D. J. NEWMAN AND J. R. POSTGATE, *Eur. J. Biochem*, 7 (1968) 45

105   G V. NOVIKOV, L. A. SYRTSOVA, G I. LIKHTENSHTEIN, V. A TRUKHTANOV, V. F. RACHEK AND V. I. GOL'DANSKII, *Dokl. Phys Chem. Proc. Acad. Sci. USSR (English Translation)*, 181 (1968) 590.

106   W. H. ORME-JOHNSON AND H BEINERT, *Biochem Biophys. Res Commun.*, 36 (1969) 337.

107   W. H. ORME-JOHNSON, R E HANSEN AND H BEINERT, *Federation Proc* 27 (1968) 298

108   W H. ORME-JOHNSON, R E HANSEN, H. BEINERT, J C. M. TSIBRIS, R C BARTHOLOMAUS AND I. C. GUNSALUS, *Proc Nat Acad Sci U S.*, 60 (1968) 368

109   G. PALMER, *Biochem Biophys. Res. Commun*, 27 (1967) 315.

110   G. PALMER AND V. MASSEY, *J. Biol. Chem*, 244 (1969) 2614

111   G. PALMER AND R. H. SANDS, *J. Biol Chem*, 241 (1966) 253.

112   G. PALMER, R C. BRAY AND H. BEINERT, *J. Biol. Chem*, 239 (1964) 2657.

113   G. PALMER, R. H. SANDS AND L. E. MORTENSON, *Biochem. Biophys. Res. Commun*, 23 (1966) 357.

114 G. Palmer, H Brintzinger and R. W. Estabrook, *Biochem.*, 6 (1967) 1658.
115 G. Palmer, H. Brintzinger, R W. Estabrook and R. H. Sands, in A. Ehrenberg, B G. Malmström and T Vanngard (Eds), *Magnetic Resonance in Biological Systems*, Pergamon Press, London, 1967, p. 159.
116 W. D Phillips, E. Knight, Jr , and D C. Blomstrom, in A. San Pietro (Ed.), *Non-Heme Iron Proteins*, Antioch Press, Yellow Springs, Ohio, 1965, p 69.
117 J A. Peterson and M. J. Coon, *J Biol Chem*, 243 (1968) 329.
118 M, Poe, W. D. Phillips, C. C McDonald and W. Lovenberg, *Proc Nat. Acad Sci. U S*, 65 (1970) 797.
119 K. V. Rajagopalan and P Handler, *J. Biol. Chem*, 239 (1964) 1509.
120 K. V. Rajagopalan, P. Handler, G. Palmer and H. Beinert, *J. Biol. Chem*, 243 (1968) 3784
121 K. V. Rajagopalan, P. Handler, G. Palmer and H. Beinert, *J. Biol. Chem*, 243 (1968) 3797.
122 R. H. Sands, in P G Debrunner, J. C. M. Tsibris and E. Munck (Eds), *Mossbauer Spectroscopy in Biological Systems*, Engineering Experimental Station, University of Illinois, Urbana, 1969, p 16
123 R H. Sands, private communication (1969).
124 R. A. Schunn, C J. Fritchie and C T Prewitt, *Inorg. Chem*, 5 (1966) 892
125 Y I. Shethna, P. W. Wilson, R. E. Hansen and H Beinert, *Proc. Nat Acad Sci U S*, 52 (1964) 1263.
126 Y. I. Shethna, P. W. Wilson and H Beinert, *Biochim Biophys Acta*, 113 (1966) 225.
127 L C. Sieker and L. H Jensen, *Biochem Biophys. Res Commun*, 20 (1965) 33.
128 G A Slack, F. S. Ham and R M Chrenko, *Phys. Rev*, 152 (1966) 376
129 B. E. Sobel and W. Lovenberg, *Biochem*, 5 (1966) 6
130 G. Strahs and J. Kraut, *J. Mol. Biol*, 35 (1968) 503
131 K. Sugeno and H. Matsubara, *Biochem Biophys. Res. Commun*, 32 (1968) 951.
132 K. Suzuki and T Kimura, *Biochem Biophys. Res. Commun*, 28 (1967) 514.
133 K. Tagawa and D. I. Arnon, *Nature*, 195 (1962) 537
134 K Tagawa and D I Arnon, *Biochim Biophys. Acta*, 153 (1968) 602
135 M. Tanaka, A. M. Benson, H. F. Mower and K. T. Yasunobu, in A. San Pietro (Ed), *Non-Heme Iron Proteins*, Antioch Press, Yellow Springs, Ohio, 1965, p 221.
136 M. Tanaka, T. Nakashima, A Benson, H Mower and K T. Yasunobu, *Biochem*, 5 (1966) 1666
137 J T Thomas, J H. Robertson and E G. Cox, *Acta Cryst*, 11 (1958) 599
138 J H. M Thornley, J. F Gibson, F. R Whatley and D. O. Hall, *Biochem. Biophys. Res. Commun*, 24 (1966) 877
139 R. L. Tsai, J. C. M. Tsibris, I. C. Gunsalus, W. H. Orme-Johnson R E. Hansen and H Beinert, (1970) in preparation.
140 J. C. M. Tsibris and I. C Gunsalus, (1968) unpublished results
141 J. C. M. Tsibris, R L. Tsai and I. C. Gunsalus, (1967), *Abstracts 154th National Meeting*, American Chemical Society, Chicago, C204
142 J. C. M. Tsibris, R. L. Tsai, I C. Gunsalus, W. H Orme-Johnson, R. E Hansen and H. Beinert, *Proc Nat. Acad. Sci. U S.*, 59 (1968) 959.
143 J. C. M. Tsibris, M. J. Namtvedt and I C Gunsalus, *Biochem Biophys Res. Commun*, 30 (1968) 323.
144 J. N. Tsunoda, K. T Yasunobu and H. R. Whiteley, *J Biol Chem*, 243 (1968) 6262.
145 D. D. Ulmer and B L. Vallee, *Biochem*, 2 (1963) 1335.
146 M. Van De Bogart and H Beinert, *Anal Biochem*, 20 (1967) 325
147 C. H. Wei and L F Dahl, *Inorg Chem*, 4 (1965) 1.
148 C H. Wei, G. R. Wilkes, P. M Treichel and L F. Dahl, *Inorg. Chem.*, 5 (1966) 900.
149 B. Weinstein, *Biochem Biophys Res Commun*, 35 (1969) 109.
150 H. H. Wickman, M. P. Klein and D. A. Shirley, *J. Chem. Phys*, 42 (1965) 2113.
151 D. F Wilson, *Arch Biochem Biophys*, 122 (1967) 254
152 G. S. Wilson, in P G. Debrunner, J. C. M. Tsibris and E Munck (Eds), *Mossbauer Spectroscopy in Biological Systems*, Engineering Expt. Station, University of Illinois, Urbana, 1969, p. 20

153   R. W. WOODY, J. C. M. TSIBRIS AND I. C. GUNSALUS, (1970) in preparation
154   C. S. YANG AND F. M. HUENNEKENS, *Biochem. Biophys. Res Commun.*, 35 (1969) 634.
155   C.-A. YU AND I C. GUNSALUS, in P G. DEBRUNNER, J C M. TSIBRIS AND E. MUNCK (Eds.),
       Mossbauer Spectroscopy in Biological Systems, Engineering Expt. Station, University of
       Illinois, Urbana, 1969, p. 68.